ÉCOLE DE TECHNOLOGIE SUPÉRIEURE
UNIVERSITÉ DU QUÉBEC

THESIS PRESENTED TO
ÉCOLE DE TECHNOLOGIE SUPÉRIEURE

IN PARTIAL FULFILLMENT OF THE REQUIREMENTS FOR
A MASTER'S DEGREE IN AUTOMATED MANUFACTURING ENGINEERING
M. Eng.

BY
Jean-François CHARRON

# VACUUM INFUSED ANIONIC POLYAMIDE-6 COMPOSITES: A QUEST FOR UNIFORMITY

MONTREAL, APRIL 26, 2011

# BOARD OF EXAMINERS

THIS THESIS WAS EVALUATED

BY THE FOLLOWING BOARD OF EXAMINERS

Mr. Simon Joncas, ing. Ph.D., Thesis director
Département de génie de la production automatisée à l'École de technologie supérieure

Mr. Henri Champliaud, ing., Ph.D., Thesis co-director
Département de génie mécanique à l'École de technologie supérieure

Mr. Michel Rioux, Ph.D., President of the Board of Examiners
Département de génie de la production automatisée à l'École de technologie supérieure

Mme. ir. Julie J.E. Teuwen, External examiner
Faculteit Luchtvaart- en Ruimtevaarttechniek at the Technische Universiteit Delft, Delft, Nederland

THIS DISSERTATION WAS PRESENTED AND DEFENDED

BEFORE A BOARD OF EXAMINERS AND PUBLIC

ON MARCH 8 2011

AT ÉCOLE DE TECHNOLOGIE SUPÉRIEURE

# FOREWORD

This thesis follows the work done during my last bachelor degree internship. For this internship, I was hired as a research assistant at the DPCS group of the TU Delft (Nederland). Over there, I was introduced to reactive infusion of anionic polyamide-6 (APA-6) composites. I truly believe that APA-6 composites have a high development potential for many application, such as wind turbine blade structures. For this reason, I did a thesis related to this subject.

The work presented in this thesis results from a collaboration between the École de technologie supérieure and TU Delft. As an exchange program master student, I went back to TU delft to follow lectures on composite materials and to complete experiments on APA-6 composites. I chose to write this thesis in English (although the Québec population granted most of my tuition fees) because one of the jury members is not a francophone. Furthermore, this thesis should be more accessible to the community of APA-6 composites researchers since it is written in English.

Part of this master degree, a paper was publish at the Twenty-Fourth Technical Conference of the American Society for Composites:

Charron, J.-F. *et. al.* 2009. “Vacuum infused anionic polyamide-6 composites: A comparison study between different mould heating strategies” *Proceedings of the American Society for Composites: Twenty-Fourth Technical Conference*, Newark, DE, September 15–17, 2009. American Society for Composites, CD-ROM-16 pp.

# ACKNOWLEDGEMENTS

I would like to thank all the people that help me out through this master degree.

First, my director, S. Joncas, ing. Ph.D., and my former supervisor, Dr.ir. K. van Rijswijk, for introducing me into the world of APA-6 in 2005. Without them, none of this would have been possible. Miss ir. J.J.E. Teuwen for guiding me on the structure of this thesis and also to help me understand the APA-6 chemical reaction process. Also the technicians, who without them, it would have been very much more difficult, S. “surfer” Lindstedt, S. van der Meer and F. Oostrum. Furthermore, I would like to express my gratitude to Ms. L. Vollmer for being so kind with us, the exchange students. Also, for her helping hand on housing and for explaining me the principles of bike fishing. Finally, all the new friends that I have met during my stay in the Netherlands, with who I had a lot of fun to travel with or to learn their languages or cultures.

Moreover, I also would like to acknowledge my ÉTS LIMAC office mates, L. “papa” Cormier, ing. jr. M. Ing., L.-C. “camarade” Forcier, M. Ing. and M.-A. “bécyk” Beauchamps, M. Ing., for many interesting diverging office discussions. Without them this thesis would not have been done on an almost trouble-free grammar checker less typesetting free software. Thanks guys, for all the support, tips and for exterminating many LaTeX bugs.

Brüggemann Chemical (Germany) and Ten Cate Advanced Composites (Netherlands) are also acknowledged for kindly supplying the APA-6 resin and the glass fibers.

Finalement, je tiens à remercier mes parents, Priscilla et Charles, pour leur soutien moral.

# L'INFUSION SOUS VIDE DU COMPOSITE POLYAMIDE-6 ANIONIQUE : UNE QUÊTE POUR L'UNIFORMITÉ

Jean-François CHARRON

## RÉSUMÉ

Depuis peu, l'utilisation des composites thermoplastiques augmente de façon considérable puisqu'ils sont abordables, recyclables et que leurs cycles de moulage sont rapides. Dans un effort de rendre la fabrication de pièces composites thermoplastiques de grandes dimensions mieux adaptée, l'Université de technologie de Delft (TU Delft) a développé un procédé d'infusion réactif de résine polyamide-6 anionique (APA-6). Selon des travaux récents, il y a des disparités quant aux propriétés mécaniques et physiques des laminés selon le sens de l'écoulement de la résine lors de l'infusion. Les travaux de ce mémoire ont donc comme but de réduire ces disparités, rendant ainsi les laminés plus uniformes. Cela est fait par l'étude de deux montages chauffants et par l'essai d'une nouvelle stratégie d'infusion.

En premier lieu, une étude de compatibilité entre le système APA-6 et l'agent de pontage contenu dans l'ensimage propriétaire 8225 est faite. Les résultats ont démontré que cet agent de pontage est compatible avec le système d'APA-6 puisqu'il obtient de bons degrés de conversion, de cristallinité et de résistance au cisaillement interlaminaire. Cependant, il ne permet pas de meilleures performances comparativement à l'ancien agent de pontage contenu dans l'ensimage 8207 précédemment utilisé.

Une seconde étude est faite afin de comparer deux montages de chauffage : la presse conductrice et les panneaux infrarouges. Cette étude est effectuée en analysant la résistance au cisaillement interlaminaire, la cristallinité et le degré de conversion, à trois températures de polymérisation différentes (160℃, 170℃ et 180℃). Les résultats de cette étude montrent que le montage infrarouge produit de meilleurs laminés que ceux faits par la presse conductrice. Cependant, ces laminés contiennent encore les mêmes disparités mécaniques et physiques, mais ceux polymérisés à 180℃ possèdent les propriétés les plus intéressantes.

Basée sur les résultats précédents et afin de rendre les laminés uniformes, une troisième étude a été effectuée en utilisant une stratégie d'infusion à deux étapes. Une infusion de résine à faible température (110-150℃) est faite suivi de la seconde étape, la polymérisation à 180℃. Les résultats montrent que les laminés les plus uniformes sont obtenus à l'aide de la stratégie à deux étapes à des températures d'infusion entre 110℃ et 130℃. Les écarts-types de la température de fusion et de la résistance au cisaillement interlaminaire de ces laminés sont plus faibles que ceux infusés à 150℃ ou ceux fabriqués selon la stratégie non isotherme précédemment utilisé. De plus, ce gain d'uniformité a été confirmé par des tests ultrasoniques et par microscope optique.

**Mots-Clés:** Matériaux composites, polyamide, polymerisation anionique, infusion sous vide, interphase, résistance au cisaillement interlaminaire, calorimétrie différentielle à balayage

# VACUUM INFUSED ANIONIC POLYAMIDE-6 COMPOSITES: A QUEST FOR UNIFORMITY

Jean-François CHARRON

## ABSTRACT

In recent years, the use of thermoplastic composites (TPC) increased significantly because of their low cost, fast processing cycles and recyclability. In an effort to provide a manufacturing technique well suited for large TPC parts, Delft University of Technology has developed an infusion process based on a reactive anionic polyamide-6 (APA-6) resin system. Following recent work where significant differences in mechanical and physical laminates property with respect to flow direction were identified, the work presented in this thesis aims at improving laminate uniformity by testing different heating set-ups and infusion strategies.

First, the fibre coupling agent, contained in the proprietary 8225 finish, was tested to asses its compatibility with APA-6. Results show that this fibre coupling agent is compatible with the APA-6 matrix system, but is not better or worse that the previous 8207 finish used in previous work done at TU Delft.

Through a second study, key laminate properties were evaluated (ILSS, crystallinity and degree of conversion) using two different heating set-ups (platen press and infrared panels) over three different curing temperatures (160-180°C). The results of this study identified that the infrared method yielded better laminates than the platen press set-up. However, most laminate produced still had non-uniform properties with respect to flow direction, but laminates cured at 180°C showed better average properties.

Based on these results, to improve property uniformity, a third study was conducted using the double infusion strategy: a low infusion temperatures (110-150°C) followed by a curing step performed at 180°C. The results showed that the best laminate uniformity could be achieved with this double infusion strategy at infusion temperatures between 110°C and 130°C. The $T_m$ and ILSS of these laminates exhibited lower standard deviation when compared to the one infused at 150°C and the one polymerised with a non-isothermal strategy. This uniformity enhancement was also validated with comparative laminate C-scans and optical microscopy results.

**Keywords:** Composite materials, polyamide, anionic polymerisation, Thermoplastic vacuum infusion, interphase, interlaminar shear strength, Differential scanning calorimetry

# TABLE OF CONTENTS

Page

# LIST OF TABLES

Page

# LIST OF FIGURES

# LIST OF SYMBOLS

| | |
|---|---|
| $\alpha$ | Alpha-phase crystal |
| $\gamma$ | Gamma-phase crystal |
| $\Delta H_{100}$ | Fully crystalline polyamide-6 melting enthalpy [J/g] |
| $\Delta H_m$ | Specimen melting enthalpy [J/g] |
| $\Delta P/\Delta x$ | Pressure gradient [Pa/m] |
| $\Delta T_{peak}$ | Temperature difference of the exothermic peaks [°C] |
| $\mu$ | Resin viscosity [Pa·s] |
| $\upsilon_f$ | Volume fraction of fibres |
| $A$ | Cross section area [m$^2$] |
| APA-12 | Anionic polyamide-12 |
| APA-6 | Anionic polyamide-6 |
| ASTM | American Society for Testing and Materials |
| $b$ | Width of ILSS sample [mm] |
| CAS | Chemical abstracts service |
| CBT® | Cyclic butylene terephthalate |
| DAM | Dry as moulded |
| DOC | Degree of conversion [%] |
| DPCS | Design and production of composite structures |
| DSC | Differential scanning calorimetry |
| $F^{\mathrm{sbs}}$ | Short-beam strength [MPa] |
| $h$ | Thickness of ILSS sample [mm] |
| HDCL | Hexamethylene-1,6-dicarbamoylcaprolactam |
| HPA | Hydrolitic polyamide |
| IFSS | Inter facial shear strength [MPa] |

| | |
|---|---|
| ILSS | Interlaminar shear strength [MPa] |
| IR | Infrared |
| $K$ | Permeability [$\mathrm{m}^2$] |
| LIMAC | Laboratoire d'ingéniérie des matériaux composites |
| $m_f$ | Mass of residual fibre [g] |
| MgBrCL | Magnesium bromide caprolactam |
| $\bar{M}_w$ | Weight-average molecular weight |
| $m_{mon}$ | Mass of loss monomer [g] |
| MMU | Mini Mixing Unit |
| $m_{tot}$ | Mass of total sample [g] |
| NaCL | Sodium caprolactam |
| PA-6 | Polyamide-6 |
| PA-12 | Polyamide-12 |
| PBT | Polybutylene terephthalate |
| PC | Polycarbonate |
| PEEK | Polyether etherketone |
| PEI | Polyetherimide |
| PES | Polyethersulfone |
| PET | Polyethyleneteraphthalate |
| $P_m$ | Maximum load [N] |
| PMC | Polymer-matrix composite |
| PMMA | Acrylic, polymethylmethacrylate |
| PP | Polypropylene |
| PPA | Polyphthalamide |
| PPS | Polyphenylene sulfide |
| $Q$ | Volumetric flow rate [$\mathrm{m}^3/\mathrm{s}$] |

| | |
|---|---|
| RIFT | Resin infusion under flexible tooling |
| RIM | Reaction injection moulding |
| RIP | Reaction injection pultrusion |
| ROP | Ring-opening polymerisation |
| RRIM | Reinforced reactive injection moulding |
| RTM | Resin transfer moulding |
| SBS | Short-beam strength |
| SCRIMP™ | Seeman Composites Resin Infusion Manufacturing Process |
| SPrr | Set point ramp rate |
| SPS | Syndiotactic polystyrene |
| SRIM | Structural reaction injection moulding |
| $T_{crys}$ | Crystallisation temperature [°C] |
| $T_{de-block}$ | De-blocking temperature [°C] |
| $T_g$ | Glass transition temperature [°C] |
| TGA | Thermal gravimetric analysis |
| $T_m$ | Melt temperature [°C] |
| TPC | Thermoplastic composite |
| TP-RTM | Thermoplastic resin transfer moulding |
| TP-VI | Thermoplastic vacuum infusion |
| $V$ | Flow front velocity [m/s] |
| VARTM | Vacuum-assisted resin transfer molding |
| VOC | Volatile organic compounds |
| WAXS | Wide-angle X ray scattering |
| WTB | Wind turbine blades |
| $X_c$ | Degree of crystallinity [%] |

# INTRODUCTION

Nowadays, environment protection is a big concern. A great example of this is the adoption of legislation L 269/34 of the European Parliament and the Council of the European Union dealing with the end-of-life of vehicles [1]. This legislation clearly promotes the conservation and protection of the environment. It states that by 2015, vehicles sold on European soil must be at least 85% recyclable by average weight. Consequently, the automotive industry was forced to take action to gradually replace thermosetting reinforced plastics used in their vehicles with reinforced engineering thermoplastics, which are recyclable. Although not bound by any legislation yet, the aerospace industry, always keen on using high-performance materials, is also gradually switching to high-performance thermoplastic composites instead of thermosetting composites. In general, thermoplastics have better dielectric properties, chemical resistance, fracture toughness, fire resistance and can offer faster processing cycles when compared to conventional thermosetting plastics [2].

Moving away from thermosetting polymers towards thermoplastic polymers forces manufacturers to adopt completely new moulding methods. Thermoplastic composite (TPC) manufacturing processes are usually classified in two groups: melt processes and reactive processes. The melt processes generally ask for expensive tooling and equipment such as presses, autoclaves and/or fibre placement machines. Furthermore, the dimensional limitations of the presses or autoclaves limit the size of TPC parts that can be produced. Consequently, melt processes can only produce small to medium-sized parts. To produce medium to large-sized parts, reactive processes such as thermoplastic resin transfer moulding (TP-RTM) or vacuum infusion processes can be used. In that respect, Verrey's work [3] has showed the feasibility of the TP-RTM on an automotive structure made of a carbon fibres and an anionic polyamide-12 resin system. Compared to TP-RTM, the vacuum infusion process has the advantage of only using one rigid mould and a flexible bag, which can significantly reduce tooling cost. The vacuum infusion process is also a process of choice to produce boat hulls and wind turbine blades (WTBs) [4].

Van Rijswijk [5] reviewed different thermoplastic systems suitable for the infusion of large structures like WTBs. He concluded that anionic polyamide-6 (APA-6) is the most promising system. Therefore, a large research program was started on the subject at the Design and Production of Composite Structures group of the Delft University of Technology. In recent years, van Rijswijk [6] and Pillay [7] have demonstrated that it is possible to produce APA-6 composites with glass or carbon fibres using this infusion process.

Nevertheless, the work of Teuwen [8] and van Rijswijk [9] has shown that APA-6/glass laminates can exhibit significantly non uniform properties over their surface. Relatively large differences in mechanical and physical properties such as interlaminar shear strength (ILSS), degree of crystallinity ($X_c$) and void content were observed with respect to resin flow direction.

**Thesis outline**

This thesis is part of the work of Design and Production of Composite Structures group of the Delft University of Technology towards manufacturing wind turbine blades made with polyamide-6. The aim of the present work is to reduce these large property variations within a laminate. This thesis contains five chapters.

Chapter 1 presents a literature review on composite materials, a brief overview of wind turbine blade composite manufacturing processes and finally, the anionic polyamide-6 resin system and its composite. Chapter 2 explains the experimental process, materials and tests methods involved in making and analysing APA-6 laminates.

Chapter 3 investigates the compatibility of a new fibre glass surface finish with the APA-6 matrix system. The glass fibre supplier of the DPCS group stopped producing the 8207 finish used for previous work. Instead, this supplier coats their glass fibres with a new 8225 finish, which is said to be compatible with polyamides. Unfortunately, the coupling agent in the 8225 finish is unknown. Therefore, a benchmark study will be presented to find out if this unknown coupling agent is compatible with the APA-6 system, and if so, to evaluate if it is better than its predecessor, the 8207 finish.

Chapter 4 presents a benchmark study between two heating set-ups: the platen press set-up and the radiative set-up. One of the reasons van Rijswijk *et al.* were unable to produce uniform composites while maintaining its (ILSS) properties was because of the too low heating rate capability of the platen press used. Also, the dimensions of the platen press is suspected to be too small to effectively heat the entire surface of the laminate to be infused. Thus, a new radiative set-up made of infrared lights providing a higher heating rate and larger coverage was tried and compared with the platen press set-up.

Chapter 5 presents the results of a study about the infusion strategy developed to improve laminate uniformity while maintaining its properties. This infusion strategy involves the heating set-up which produces the best laminates from the study of chapter 4. The novel infusion strategy is the double step strategy which consists of infusing the laminate with an infusion temperature lower than the polymerisation temperature.

Finally, conclusions and recommendations are made for future research.

# CHAPTER 1

# LITERATURE REVIEW

## 1.1 Introduction to composite materials

As the name suggests, a composite material is composed of at least two distinct material united. Typically, it is composed of two phases, a non continuous phase, like a fibre or a particle, which is generally stiffer and stronger than the continuous phase, the matrix. This matrix can be of metallic, ceramic or organic nature, which includes the polymer-matrix composite (PMC) class.

The overall PMC properties are driven by the properties of the fibres and matrix, their volume ratios and the architecture or orientation of the reinforcing fibres. The main reason why composite materials are used is because of the possibility they offer to obtain higher specific modulus and specific strength, when compared to classic isotropic materials.

Because this work is about PMC, only this class of composite will be discussed.

### 1.1.1 PMC reinforcements

Many reinforcements can be used in a PMC, however, to produce an efficient PMC, it is advised to use a volume ratio of reinforcement/PMC of at least 10%. Furthermore, these reinforcements can be of different form, nature, and architecture. That is why it is so important to select them with care to achieve the desired properties at a reasonable cost.

Spheres, rods, flakes, and whiskers can be used as discontinuous reinforcements. They are usually used to “fill” the matrix for non-structural purposes such as fire resistance, control of shrinkage, increase of thermal or electrical conductivity or even to lower the part cost. For structural purposes, continuous fibre reinforcements are generally used, which provide virtually all of the strength and stiffness in a continuous fibre-reinforced composite.

After the proper reinforcement form selection, it is time to select its nature. Many natures of reinforcement are used in a PMC. The most widely used reinforced fibres for a PMC are glass, carbon and aramid fibres. Because this work is related to glass fibre, only this fibre will be discussed. Here are some of the advantages glass fibre can offer:

- excellent mechanical performance/cost ratio,
- good adhesion to matrix due to different coupling agents,
- good hygrothermal resistance,
- low thermic dilatation & conductibility,
- good dielectric property.

Nowadays, to minimize the cost of the electricity produced by large wind turbines, their blades are mainly made of low cost glass fibres.

The simplest architecture of the reinforcement is the single fibre. It can be transformed into multiple forms such a strand, which includes thousand of monofilaments put together. Again, strands can be put together to form rovings. From rovings more complex architectures can be made like tapes, brands and woven rovings. Each of these types of materials have their advantages and properties. To get the best performance from a PMC structure, it is recommended to use a combination of different reinforcement architectures. In the case of wind turbine blades, they are usually made from unidirectional fabric and woven roving fabric [10–12].

### 1.1.2 PMC matrices

The matrix of a PMC is of course a polymer as previously explained in section 1.1. A polymer is the product of a polymerisation process during which polymer chains are created. These chains are large molecules made of small molecules called monomers. The

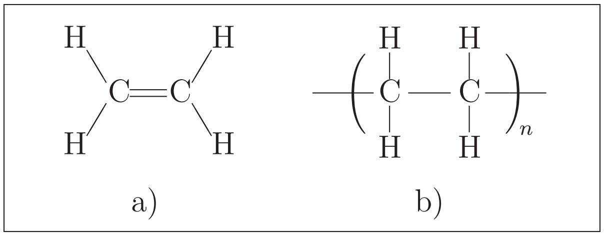

Figure 1.1 a) Polyethylene monomer & b) repeating unit.

final properties of the polymer are driven by the properties of the monomer initially used. The name of many polymers comes from the name of the monomer with the suffix poly-. As an example, figure 1.1a) shows the ethylene monomer and polymer form (repeating unit), which is called a polyethylene chain in figure 1.1b).

In a PMC, the polymer plays many roles. By its cohesive and adhesive characteristics, the polymer holds the reinforcements together in the desired orientations. Consequently, load transfer between the matrix and reinforcements is made possible. The polymer drives also the stiffness and the strength of a PMC at high temperature. Above the polymer's glass transition temperature, $T_g$, the properties of the PMC will change drastically. For most polymers, properties like stiffness and strength will significantly decrease above the $T_g$. The polymer also protects the PMC part from the environment since it is the polymer that comes first in contact with solvents, abrasive surfaces or other environmental hazards. Therefore, polymer selection has to be done properly to guarantee that the PMC part will perform as desired.

There are two categories of polymer matrices: thermosetting matrices and thermoplastic matrices. These two categories will be reviewed in the next two sections.

#### 1.1.2.1 Thermosetting matrices

Thermosetting polymers are characterized by the 3D unmodifiable molecule network made after the polymerisation completion. A PMC made of a thermosetting plastic cannot be remoulded or recycled by melting. This is due to the two stages involved in

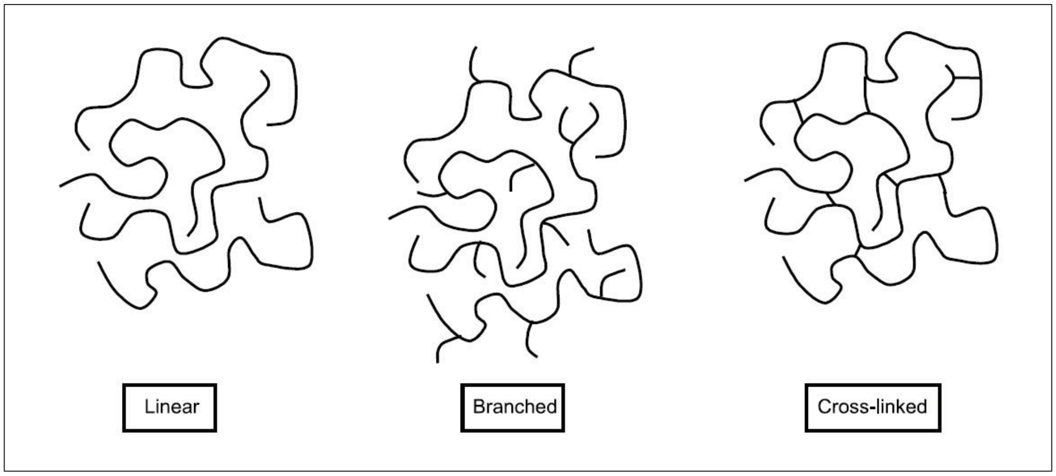

Figure 1.2 Linear, branched and cross-linked polymer structures. From [13, p.54]

their polymerisation process. First, the monomers unite together to form long molecular chains. Then, these chains are tied together by strong covalent bonds, called cross-links. This turns the polymer into a 3D network of long molecular chains, as illustrated in figure 1.2. Because of these cross-links, even if heat is applied to the polymerised thermosetting plastic, it will not be possible to soften it. Ultimately, if too much heat is applied, the polymer will simply be scorched.

The three most common thermosetting polymers used in today's industries are polyesters, vinyl esters and epoxies. In general, polyester matrices are use in low cost applications. The vinyl ester are well known for corrosive applications and epoxies for structural applications. In addition, all of these matrices can be customised for different moulding processes. Often in the wind energy industry the polymers used are epoxies.

#### 1.1.2.2 Thermoplastics

The main differences between the thermoplastic and the thermosetting polymer are the remoulding, softening, and recycling capabilities they offer when heated. A thermoplastic can be remoulded because it is not cross-linked. It is either a linear or a branched structure as seeing in figure 1.2. The thermoplastics also have other advantages like

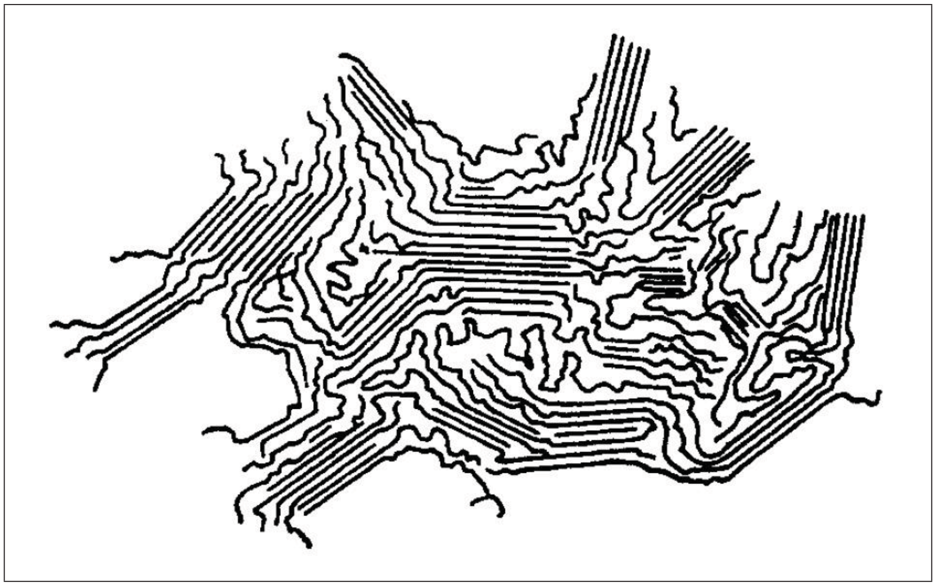

Figure 1.3 Planar zigzag representation of molecules in a semi-crystalline polymer. From [14, p.50]

being tougher, having longterm room-temperature storage (better shelf life) and having higher strains-to-failure when compared to thermosetting polymers.

A linear or branched thermoplastic can be either an amorphous or a semi-crystalline polymer. An amorphous polymer has its molecular chains displayed in random, non-organised manner. In other words, an amorphous polymer would look like a plate of spaghetti under the microscope. In opposition, semi-crystalline polymers have well organised polymer chains to create crystals. These polymer chains are crystallised in a spiral or planar zigzag as seeing in figure 1.3. Amorphous and semi-crystalline polymers have different characteristics due to their different molecular arrangements. Table 1.1 shows the typical characteristic of these two types of thermoplastic.

Figure 1.4 classifies different thermoplastics by their molecular arrangement and typical commercial applications. The advanced engineering class is also known as high performance plastics. The thermoplastics that do not resist well to heat are shown at the bottom of the pyramid and the one which resist well to heat are place at the top of

Table 1.1 Typical characteristics of amorphous and semi-crystalline plastics
Adapted from [15, p.4-5]

| Characteristics | Amorphous | Semi-crystalline |
|---|---|---|
| Fusion | **Broad softening range**: thermal agitation of the molecules breaks down the weak secondary bonds. The rate at which this occurs throughout the formless structure varies producing broad temperature range for softening. | **Sharp melting point**: the regular close-packed structure results in most of the secondary bonds being broken down at the same time. |
| Color | **Usually transparent**: the looser structure transmits light so the material appears transparent. | **Usually opaque**: the difference in refractive indices between the two phases (amorphous and crystalline) causes interference so the material appears translucent or opaque. |
| Chemical resistance | **Low**: the more open random structure enables chemicals to penetrate deep into the material and to destroy many of the secondary bonds. | **High**: the tightly packed structure prevents chemical attack deep within the material. |
| Shrinkage | **Low**: all thermoplastics are processed in the amorphous state. On solidification, the random arrangement of molecules produces little volume change and hence low shrinkage. | **High**: as the material solidifies from the amorphous state the polymers take up a closely packed, highly aligned structure. This produces a significant volume change manifested as high shrinkage. |
| Fatigue and wear resistance | **Poor**: the random structure contributes little to fatigue or wear properties. | **Good**: the uniform structure is responsible for good fatigue and wears properties. |

the pyramid. Generally, the cost of the thermoplastics also rises with the thermal and mechanical properties. Therefore, figure 1.4 also shows thermoplastics from the least expensive to the most expensive.

### 1.1.3 Composite interface and interphase

Whatever the PMC reinforcement form or nature, an interface and interphase will always exist between the fibres and matrix. As Drzal [16] suggests, an optimized bonding interface is necessary for the composite to achieve environmental resistance and maximum

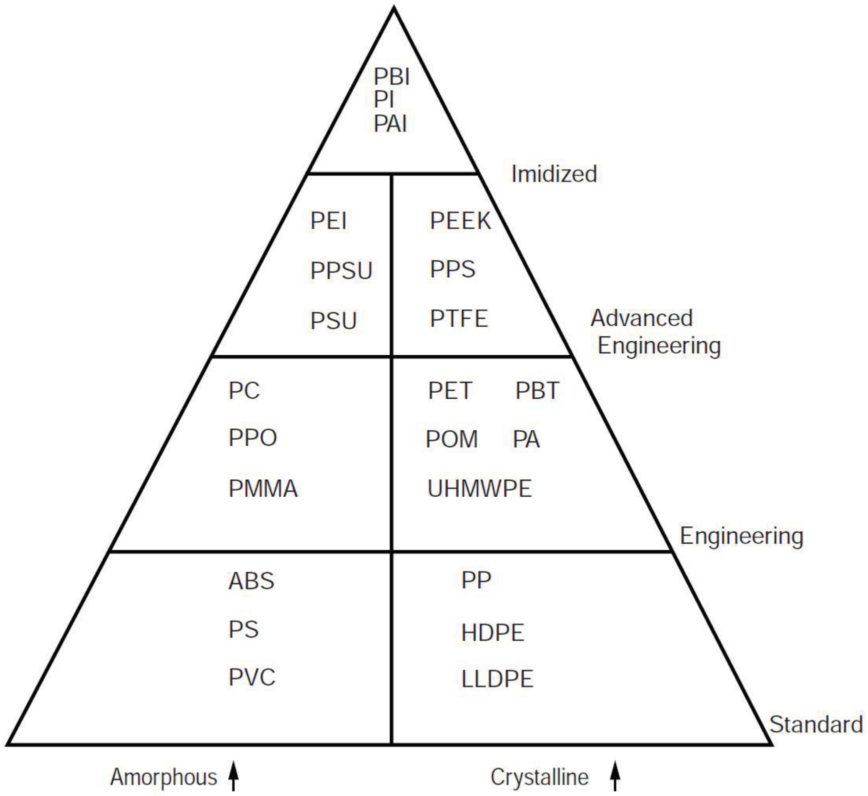

| Abbreviation | Material Name |
|---|---|
| PBI | Polybenzimidazole |
| PI | Polyimide |
| PAI | Polyamide-imide |
| PEEK | Polyetheretherketone |
| PPS | Polyphenylene Sulfide |
| PTFE | Polytetrafluroethylene |
| PEI | Polyethermide |
| PPSU | Polyuphenylsulfone |
| PSU | Polysulfone |
| PET-P | Polyethylene Terephthalate |
| PBT | Polybutylene Terephthalate |
| PA | Polyamide (Nylon) |
| POM | Polyoxmethylene (Acetal) |

| Abbreviation | Material Name |
|---|---|
| UHMWPE | Ultra High Molecular Weight Polyethylene |
| PC | Polycarbonate |
| PPO | Polyphenylene Oxide |
| PMMA | Polymethylmethacrylate (Acrylic) |
| PP | Polypropylene |
| HDPE | High Density Polyethylene |
| LDPE | Low Density Polyethylene |
| ABS | Acrylonitrite Butadience Styrene |
| PS | Polystyrene |
| PVC | Polyvinyl Chloride |

Figure 1.4 Classification of thermoplastics.
From [13, p. 8.13]

static and dynamic mechanical properties by load transfer form the fibres to the matrix and *vice versa*. To understand how the interaction between the fibre and the matrix works, a 3 dimensions interphase model has been develop by Drzal [17]. He defines the interphase as “some point in the fibre where the local properties begin to change from the

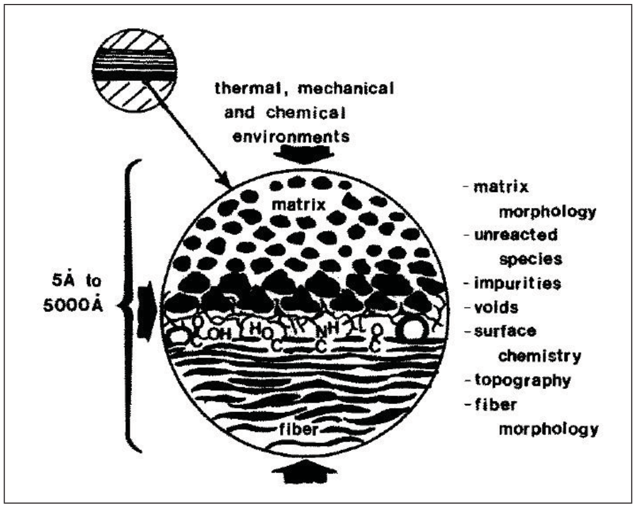

Figure 1.5 Schematic diagram of the fibre-matrix interphase.
From [16]

fibre bulk properties, through the actual interface into the matrix where the local properties again equal the bulk properties" of the matrix [16]. This interphase is illustrated in figure 1.5.

Because the structure of the interphase has a profound effect on the composite performance (mechanical strength, chemical and thermal durability, etc.) work has being done to develop coupling agents for a large number of PMC. A coupling agent is composed of chemical molecules which connect the fibre surface to the matrix using there respective reactive groups. Most of the coupling agents develop today for glass fibres are from the silane class and are compatible with most common matrix (polyester and epoxy) [18]. These coupling agents are contained in the fibre finish[1] surface treatment, which is apply to the fibres after their creation. The reader is invited to read Owen's [20], Kim & May's [18], Ranney *et al.* [21] and Plueddemann's [22, 23] work for more information on coupling agents.

---

[1] "A mixture of materials for treating glass or other fibres. It contains a coupling agent to improve the bond of the resin to the fibre, and usually includes a lubricant to prevent abrasion, as well as a binder to promote strand integrity." Unlike a finish, a size contains no coupling agent. [19, p.11 & p. 21]

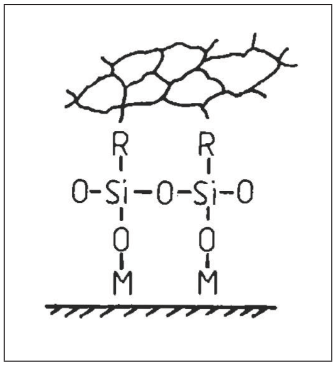

Figure 1.6 Coupling agent bonded to glass surface and organofunctional R-group reacted with polymer.
From [18, p.177]

There are many ways to directly quantify the properties and performances of the interface. The fibre pull-out, microbond, single-fibre fragmentation and microindentation tests are a few examples. An inter-laboratory test program was done to evaluate these tests [24]. The conclusion of this program state that each method tested gave a different value of the interfacial shear strength (IFSS) with values varying up to a factor of 2.7 [18, p.59]. Other indirect (qualitative) methods can be used to determine the interphase property and performance. From the mechanical property of the in-plane shear strength, transverse tensile strength and the interlaminar shear strength (ILSS), it is possible to evaluate the quality of the bond between the fibre and the matrix. The most widely used method is the ILSS because of its simplicity. The composite ILSS test is known in practice as the short-beam shear (SBS) test standardised by ASTM D 2344 (2000 and reapproved in 2006). This test does not only evaluate the composite interface performance but the overall symbiosis performance of the fibre, matrix and coupling agent mixture [16]. As explained in section 2.4.3, it is the SBS test which will be used to evaluate the ILSS of the APA-6 laminates of this thesis.

### 1.1.4 Composite manufacturing processes

To create a PMC, a manufacturing process has to be used. There are many different types of moulding processes and each type has its own variants. The moulding process

Table 1.2 Comparison of different cost categories for different manufacturing processes
Adapted from [25, p.1188]

| **Cost requirements** | **Vacuum infusion** | **RTM** | **Hand lay-up** | **Spray-up** | **Low P/T prepreg** | **Autoclave prepreg** |
|---|---|---|---|---|---|---|
| Workshop requirements | \$\$ | \$\$ | \$\$\$\$ | \$\$\$\$ | \$\$\$ | \$\$\$ |
| Equipment | \$\$ | \$\$\$ | \$ | \$\$ | \$\$\$ | \$\$\$\$\$ |
| Tooling | \$\$ | \$\$\$\$ | \$\$ | \$\$ | \$\$ | \$\$\$ |
| Ancillary materials | \$\$\$ | \$\$ | \$ | \$ | \$\$\$ | \$\$\$ |
| Raw materials | \$\$ | \$\$ | \$\$ | \$ | \$\$\$ | \$\$\$\$ |
| Labour | \$\$ | \$ | \$\$ | \$ | \$\$\$ | \$\$\$ |
| Total cost | 13×\$ | 14×\$ | 12×\$ | 11×\$ | 17×\$ | 21×\$ |

has to be chosen according to different criteria. These criteria are driven by the part size and shape, mechanical/thermal properties, series to produce and cost. Some processes ask for more equipment, less raw materials or are more labour intensive. To give a general idea, table 1.2 presents a few moulding processes with there respective cost requirements. The vacuum infusion is a low cost process which can be applicable to the WTB.

To conclude section 1.1, it is important to remember that an optimum PMC is created from the right constituents (fibres and polymer), the best achievable interphase (the bonding compatibility of the polymer to the fibres), the use of the proper process in combination with the an optimal design. This is resumed by Beukers & Hinte's engineering philosophy: the trinity essence, see figure 1.7 [26, p.22], and should be followed by engineers who wish to produce “la crème de la crème” engineered parts.

## 1.2 Today's wind turbine blade manufacturing processes

This section presents how WTB are manufactured.

Up until 1990-1995, WTBs were made with the hand lay-up process, as shown in figure 1.8a). Afterwards, to improve rotor blade performance and environmental working

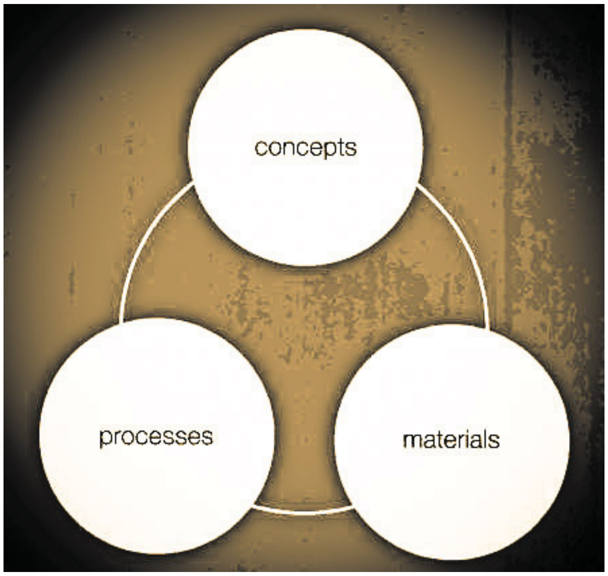

Figure 1.7 The trinity essence.
Adapted from [26, p.22]

conditions, WTB manufacturers began to search for alternative manufacturing processes. A lot of different molding processes have been investigated such as resin transfer moulding (RTM), filament winding, vacuum infusion, pre-impregnated and novel thermoplastic technologies. In the end, mainly due to cost issues, today's most widely used technologies are vacuum infusion and pre-impregnated technologies of thermosetting matrices [27–31]. The vacuum infusion process is shown on the figure 1.8b) & 1.8c) where the resin is actually shown flowing in the reinforcement. Griffin and Ashwill do not consider thermoplastics matrices promising for large wind turbine blade application because of their bonding difficulties, creep behaviour and their higher cost estimate related to baseline thermosetting matrices [28]. However, Araj *et al.* said that the full potential of polyamide and PET pre-preg were not realised because of lack of low-cost manufacturing technique [32].

It is because of this lack of low cost manufacturing techniques that the TP-VI process was preferred for the work presented in this thesis. It is believed that the combination of TP-VI with the APA-6 resin system will help to solve the problems mentioned by Griffin, Ashwill and Araj.

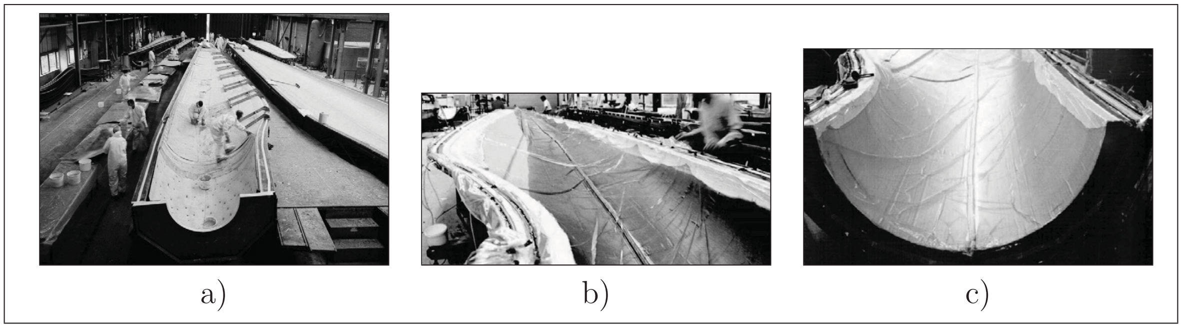

Figure 1.8 WTB manufacturing processes;
a) hand lay-up [33]
b) & c) vacuum infusion [4]

## 1.3 Vacuum infusion process

This section presents the vacuum infusion process in general because of its similarities with the one used in this thesis (later discussed in section 2.3.3).

The vacuum infusion process was mostly developed by the naval industries to replace the hand lay-up process, which was the first method used to manufacture large parts like boat hulls. One big concern of the hand lay-up process was the staff environmental working conditions. While working, these workers were exposed to too much volatile organic compounds (VOC) from the uncured resin in the mould. Also, boat builders wanted to be able to cost efficiently manufacture larger parts. Therefore, for these two reasons, the naval industries searched for alternative processes. As early as 1950, a patent was registered as the Marco method [34] and investigations continued until now to lead to the vacuum infusion family processes as we know it. The interested reader is referred to Williams *et al.* [35] where the complete vacuum infusion story is well reviewed.

The vacuum infusion family includes a lot of variants like the vacuum-assisted resin transfer molding (VARTM), resin infusion under flexible tooling (RIFT) and Seeman Composites Resin Infusion Manufacturing Process (SCRIMP™), just to name a few. All the different names and related variants are well described by Cripps *et al.* [36]. Even

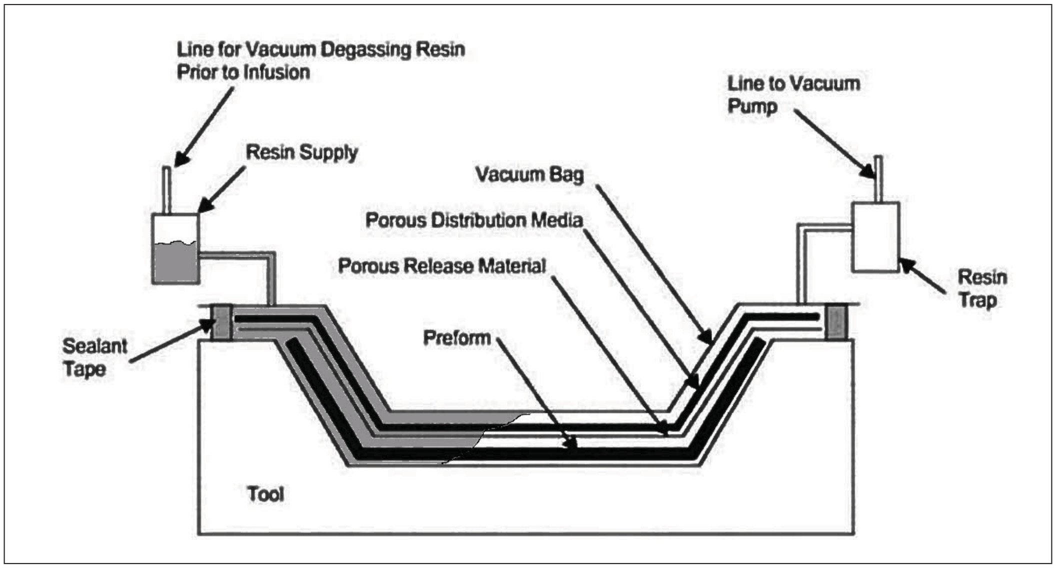

Figure 1.9 The vacuum infusion process.
Adapted from [37, p.349]

if there is 14 reported kinds of methods within the vacuum infusion family, there are similarities between them. All are derived from RTM, where one rigid mould (mostly the male mould) is replaced by a flexible mould (a film or a light tool).

To set-up an infusion moulding, dry reinforcement fabrics are first placed in the mould. Then most of the time, a peel-ply and a flow medium are positioned on top of the fabric before closing by mould with a vacuum bag. By vacuuming, the air is removed from the set-up and the laminate is compressed; the resin is now ready to flow and fill up the dry fibre bed. As seen in figure 1.9, the resin flows from the resin bucket, which is at atmospheric pressure, to the resin trap, which is under vacuum. The flow is stopped when the mould is filled (when there is no more dry fabric spot) by closing the resin inlet tube.

The driving force applied to the resin comes from the pressure difference between the inlet tube (resin bucket) and outlet tube (pressure applied by the vacuum pump). With Darcy's law (shown in equation 1.1) it is possible to understand the physics behind the infusion process [38, 39].

$$\frac{Q}{A} = V = \frac{K\ \Delta P}{\mu\ \Delta x} \tag{1.1}$$

In Darcy's law many parameters affect the resin flow front. The volumetric flow rate, $Q$ [m$^3$/s], of the resin which pass through the cross section area, $A$ [m$^2$], can be directly linked to the flow front velocity, $V$ [m/s]. This velocity is function of the set-up permeability (laminate, peel-ply and flow medium), $K$ [m$^2$], the resin viscosity, $\mu$ [Pa·s], and the pressure gradient, $\Delta P/\Delta x$ [Pa/m]. It is easy to imagine that the time required to fill up the mould can be manipulated by using different kind or materials, the vacuum pressure applied by the vacuum pump and by the distance, the resin has to flow through. For example, to speed up the resin flow front (the manufacturing cycle), a less viscous resin and/or a more permeable fabric can be used. Also, setting the vacuum pump to the minimum pressure (maximum vacuum) will reduce the filling time. Finally, the infusion strategy (the distance the resin flow front has to travel) will also influence the fill-up time (exponential with respect to distance). It is interesting to realise that in theory, an infinite part can be made with the infusion process. As the Darcy's law suggest, the resin flow front will alway go forward and never stop but will slow down on its way. In practice, the infusion process is limited in time by the resin pot life[2]. Prior to the resin infusion, the resin is mixed with its catalyst/hardener and shortly begins polymerisation, as explain in section 1.1.2.1. One of the resin polymerisation consequences is an increasing viscosity, which will affect resin flow. Hence, to guarantee a good and uniform impregnation of the fibres, it is advised to select a resin with the appropriate viscosity (around 300 mPa·s) and pot life (at least one hour). With the appropriate viscosity and pot life it will be possible to fill up the mould before the gelation time[3].

Vacuum infusion has many advantages. It can be used with different low viscosity resin systems and conventional weaved and stitched fabrics. Large high-performance struc-

---

[2] The time a catalysed resin system retains a viscosity low enough to be used in processing. [40, p.771]

[3] The interval of time in connection with the use of synthetic thermosetting resins extending from the introduction of a catalyst to a liquid adhesive system until the interval of gel formation. [40, p.764]

tural components can be consistently fabricated with relatively low tooling costs (one open mould). When compared to hand lay-up, the part consistency is less sensitive to craftsmanship, and higher fibre volume fraction ($v_f \geq 45$ %) leads to improved mechanical performance with uniform microstructure and minimal void since the fabrics are impregnated under vacuum compaction. In addition, sandwich structures can be produced in a single flow process with minimum VOC emission [36].

The vacuum infusion has not just advantages but also drawbacks. This process is more complex and requires highly skilled personnel. The process is sensitive to leaks, which could disturb the flow and may result in dry spots or even lead to scrap parts. Also this process produces waste like the ancillary materials used only once (vacuum bag, peel-ply, flow medium, sealant tape and tubes). At last, only the mould side of the part will be of a good surface finish.

## 1.4 Thermoplastic composites processes

This section presents different thermoplastics composites processes since these process are relatively new to the market. Its goal is also to differentiate the reactive processes like the one used in this thesis, *i.e.* TP-VI, from the more conventional melt processes. At the end of this section, the thermoplastics which are compatible with TP-VI are shown.

Thermoplastic composites moulding is classified in two categories: the melt process and the reactive process. Both of these categories have their own advantages and drawbacks, but most of them, if not all, have one thing in common: they need external energy (heat) to mould a PMC part. The main difference between these two categories is the matrix material viscosity used in the process. As the name suggests, the melt process is based on melting a thermoplastic polymer to create a part. Above their melting temperature, thermoplastic polymers generally have high viscosity (around 1000 Pa·s). Therefore, to conform a TPC to the mould during melt processing, a high pressure device like a press or an injection machine is needed. These devices limit the dimensions a part can have. A large structure, like a 60 m WTB, can hardly be moulded by a melt process or a gigantic and expensive press would be needed. The diaphragm forming, rubber pad forming and vacuum forming, to name a few, are all thermoplastics melt processes and are reviewed by Mallon *et al.* [41]. Alternatively, to build large structures, a reactive process can be used.

### Reactive thermoplastic liquid moulding technologies

There is three main different reactive thermoplastic liquid moulding technologies: the reactive injection moulding (RIM), the reinforced reactive injection moulding (RRIM) and the structural reaction injection moulding (SRIM). These three processes have a common element; a heated monomer solution of low viscosity (around 0.05 Pa·s) fills a heated mould to finally give a moulded part by an *in situ* polymerisation. The difference between these three processes resides in the reinforcement used within the process. The RIM does not use any reinforcement. It is a neat resin casting process. The RRIM use the presence of fillers (chopped fibres, glass flakes, mica or others minerals) in the monomer solution to enhance its final mechanical properties [42]. Finally, the SRIM refers to the filling of a preform in the mould made of fibre reinforcements (mat, fabrics or unidirectional) to improve even more its mechanical properties. Figure 1.10 synthesis the RIM, RRIM and SRIM mechanical performances related to their reinforcement type.

In fact, the SRIM is similar to both RTM and vacuum infusion, the resin solution (thermoplastic or thermosetting resin) is polymerised *in situ* after flowing into a dry fibre preform to form a PMC. The complete process has to be done within the processing windows, *i.e.* while the polymerisation rate is still low or before the monomer starts to convert into a polymer, as shown on figure 1.11. The difference is that the equipment used to melt and to mix the monomer solution for the SRIM process generally has to work at higher temperatures than the equipment used for thermosetting resin systems. These similarities leads to the following acronyms: the combination of RIM with RTM gives TP-RTM [3] and RIM with vacuum infusion can be translated as thermoplastic vacuum infusion (TP-VI), both part of the SRIM technology. Because, the TP-VI can

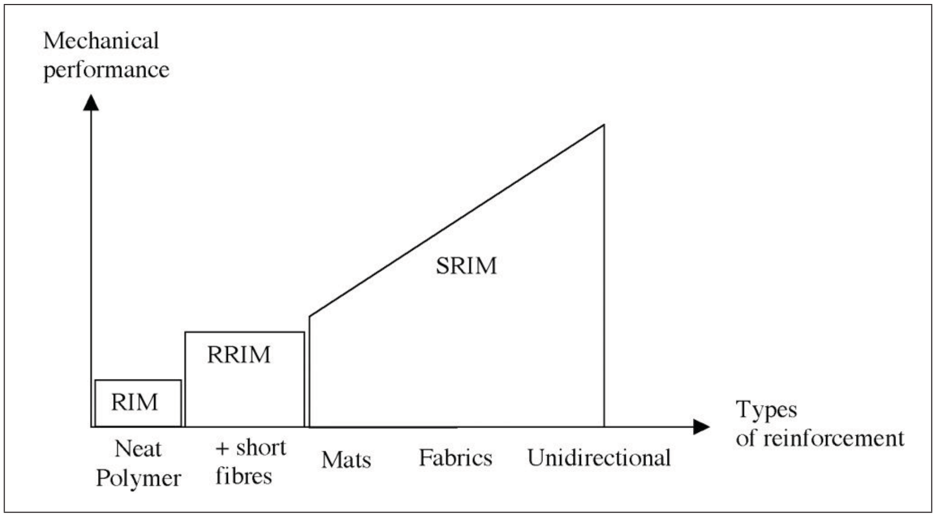

Figure 1.10 RIM, RRIM and SRIM mechanical performance related to their reinforcement type.
From [43]

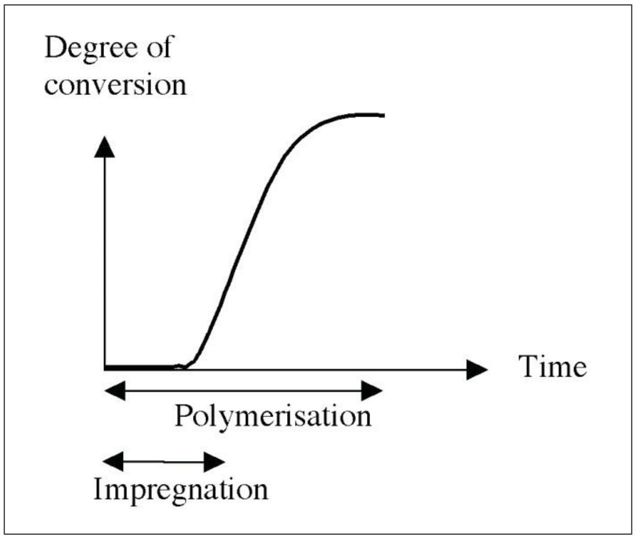

Figure 1.11 Degree of conversion *vs.* time.
From [43]

produce large parts, it is well suited to serve the wind energy industry, as explained in section 1.2.

All thermoplastics can be used for melt processing but only a few of them can be used for reactive processing. The most important reactive monomer system parameter is its viscosity. As explained in section 1.1.3, a low viscosity is needed to properly impregnated the fibres and achieve the required load transfer between the matrix and fibres. Therefore, only certain low viscosity polymer precursors (vinyl monomer, cyclic mono/oligo -mers) can be used for TP-VI when melted due to their low molecular weight. Furthermore, these precursors have to polymerise into a high molecular weight polymer with a high degree of conversion without creating unwanted byproducts. One of the most common *in situ* thermoplastic resin systems are based on ring-opening polymerisation (ROP). The ROP mechanisms are based on the opening of a cyclic monomers, M, (see equation 1.2) and on their ability to connect themselves by addition to each others, also known as the addition polymerisation (see equation 1.3).

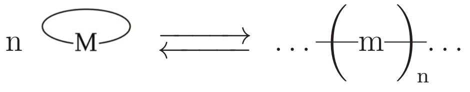

$$\text{n}\ \text{M} \rightleftarrows \ldots\!-\!\left(\!-\text{m}-\!\right)_{\text{n}}\!-\!\ldots \tag{1.2}$$

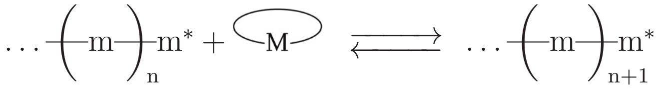

$$\ldots\!-\!\left(\!-\text{m}-\!\right)_{\text{n}}\!-\text{m}^{*} + \text{M} \rightleftarrows \ldots\!-\!\left(\!-\text{m}-\!\right)_{\text{n+1}}\!-\text{m}^{*} \tag{1.3}$$

The review paper of van Rijswijk [5] presents thermoplastics which can be polymerised by ROP (see table 1.3). Most of these thermoplastics are still in development, thus only five of them are commercially available (see table 1.4). It is interesting to notice that these five polymers have low process temperatures compared to their melt process temperatures, which consequently reduces the energy consumed during production.

The anionic polyamide-6 resin system was originally chosen because of its low viscosity, commercial availability and relatively low polymerisation temperature, see van Rijswijk for more details [52].

Table 1.3 Thermoplastic matrix processing temperature
Adapted from [5]

| **Polymers** | **Melt processing** | **Reactive processing** |
|---|---|---|
| | [°C] | |
| SPS[a] | 270 | -26 – 110 |
| TPU[b] | 200 | 70 |
| PMMA | 220 – 260 | 120 – 160 |
| PA-6 | 230 – 290 | 140 – 160 |
| PI[c] | 340 – 400 | 80 – 196 |
| PBT | 250 – 270 | 180 – 200 |
| PA-12 | 230 – 270 | 180 – 245 |
| PC | 265 – 360 | 250 |
| PPA[d] | 310 – 330 | 220 – 290 |
| PES | 330 – 390 | 300 |
| PPS | 330 | 300 |
| PEEK | 380 – 390 | 350 |

---

[a] [44]
[b] [42, p.6]
[c] [45]
[d] Research still on going to reduce the oligomer solution viscosity to 1 mPa·s range [46].

## 1.5 The anionic Polyamide 6 system (APA-6)

To help understand different concepts used throughout the remaining chapters of this thesis, this section will review the anionic polyamide 6. More specifically, the APA-6 polymer will be compared against conventional PA 6. Finally, the modifications to the original APA-6 casting system to make it suitable for a TP-VI process will be presented.

### 1.5.1 Polyamides (PA)

The APA-6 polymer is part of the polyamide family. These are engineering polymers, which contain a repeating amide group, — CONH —, in their chains and are known for their excellent load bearing (strength and stiffness) capability at elevated temperatures, good chemical and abrasion resistance, low friction coefficient, toughness, impact resistance and capabilities to be recycled [53,54]. A lot of different polyamides can be created

Table 1.4 Commercially available reactive thermoplastic systems

| **Company name** | **Commercial name** | **Polymer nature** | **References** |
|---|---|---|---|
| E.I. du Pont de Nemours and Co., Inc. | Avimid K-III & Avimid N | PI | [2, 45] |
| Cyclics Corporation | CBT® | PBT | [47] |
| Dow Plastics | Isoplast & Fulcrum™ | TPU | [48] |
| DSM & BrüggemannChemical | AP-Nylon® Materials | PA-6 | [49, 50] |
| EMS-CHEMIE AG | EMS Grivory laurylactam-12® system | PA-12 | [51] |

$$\boxed{\left( \text{NH} - (\text{CH}_2)_5 - \text{CO} \right)_n}$$

Figure 1.12 PA-6 repeating unit.

for different applications, *e.g.* PA-6, PA-12, *etc.* The way these polymers are classified is with respect to the amount of carbon atoms in their repeating units, *i.e.* PA-6 contains six carbon atoms in its repeating unit, see figure 1.12. The first polyamide, PA-66, was made in 1937 [55] and the first polyamide, PA-6, by ROP was made in 1938 [56] which make APA-6 the oldest reactive processing thermoplastic. For more informations about the history of polyamide 6, the reader is invited to read the paper of Matties *et al.* [56].

### 1.5.2 APA-6 generalities

APA-6 (also known as polycaprolactam and polycaproamide) is made from the opening of its monomer, $\varepsilon$-caprolactam shown in figure 1.13 a). $\varepsilon$-caprolactam is one of the most

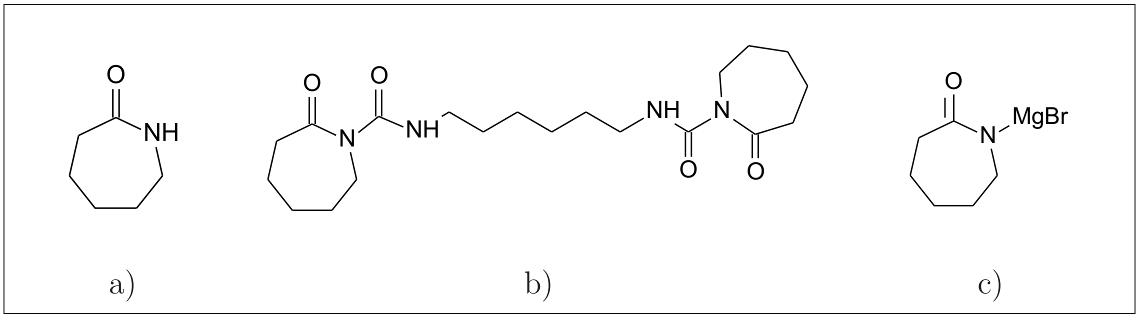

Figure 1.13 APA-6 chemicals; a) monomer: $\varepsilon$-caprolactam, b) difunctional activator: HDCL, c) initiator: MgBrCL.

studied lactam[4] if not the most. The reasons why there is so much interest and development in the field of APA-6 polymerisation is because of its much higher polymerisation rate, degree of conversion and mechanical properties [57] compared to its hydrolytic polymerisation counterpart which can take more than 24 hours to process [58]. This reaction process allows to mould more complex part below or above the PA-6 melting point ($T_m$ = 220℃). The APA-6 is often moulded under its $T_m$ because of it is more economical and because it enhances the polymer performance (crystallinity and degree of conversion) when compared to a polymer moulded above its melting point [59, 60]. Furthermore, the resulting part does not need any post moulding steps like water extraction nor post cure to produce an APA-6 part. The $\varepsilon$-caprolactam ($T_m = 69$℃) is melted and mixed with an initiator (catalyst) and an activator (co-catalyst). The polymerisation can be performed on a wide range of temperatures, between 130 – 180℃, to produce a high molecular weight polymer with conversions and crystalline content up to 99.3 % and 47 % respectively within 50 s to 60 min [57, 61]. Alkali or alkaline earth metal elements are effective initiators [62, 63], but the most commonly used initiators for APA-6 polymerisation are sodium caprolactam (NaCL) and magnesium bromide caprolactam (MgBrCL), as shown in figure 1.13 c). The latter can be made with a Grignard reagent in caprolactam [64] and give higher polymerisation rates compared to NaCL [65].

---

[4] Organic compound containing an amide group as part of a ring.

In general, the resulting APA-6 properties and kinetics are related to a few parameters. The three main parameters are the polymerisation temperature, the nature and concentration of the initiator and the nature and concentration of the activator used. Therefore, with these three parameters, the degree of crystallinity can be adapted to different applications while the kinetics are adjusted to control and suit the moulding process. For example, these parameters can be adjusted to adapt polymerisation and crystallisation rates and branching to the required filling time necessary to mould a TP-VI part. An other important APA-6 process parameter is the presence of water. It terminates the molecular chains propagation by deactivating the catalyst reaction from the activator and initiator [60, 66]. Therefore, it is necessary to store and process the chemicals in an anhydrous environment.

### 1.5.3 APA-6 polymerisation mechanisms

The APA-6 polymerisation mechanism is shown in figure 1.14. This polymerisation starts with the dissociation of the initiator to create a lactam anion, which plays the role of catalyst. Then, this anion attacks a nitrogen atom and opens a caprolactam ring of an activator via an anion exchange. This results in a chain growing from within itself and not from its end. Afterwards, the anion attacks back a monomer, which exchanges its hydrogen atom with the nitrogen anion to reach equilibrium. Ultimately, the polymer chain propagates itself until the monomers has been mostly consumed, thus the reaction stops. Consequently, it is possible that monomer remains and be trapped inside the polymer because of the monomer and polymer equilibrium at the end of the reaction.

Since the moulding temperature is within the PA-6 crystallisation temperature ($T_{crys} = 90 - 185$°C, maximum crystallisation rate = 138°C), the crystallisation occurs simultaneously with the polymerisation [67–69]. Furthermore, the APA-6 polymerisation and crystallisation are exothermic, it releases heat and create an autocatalytic effect. Therefore for large mass or thick part, it is important to take into account this released energy

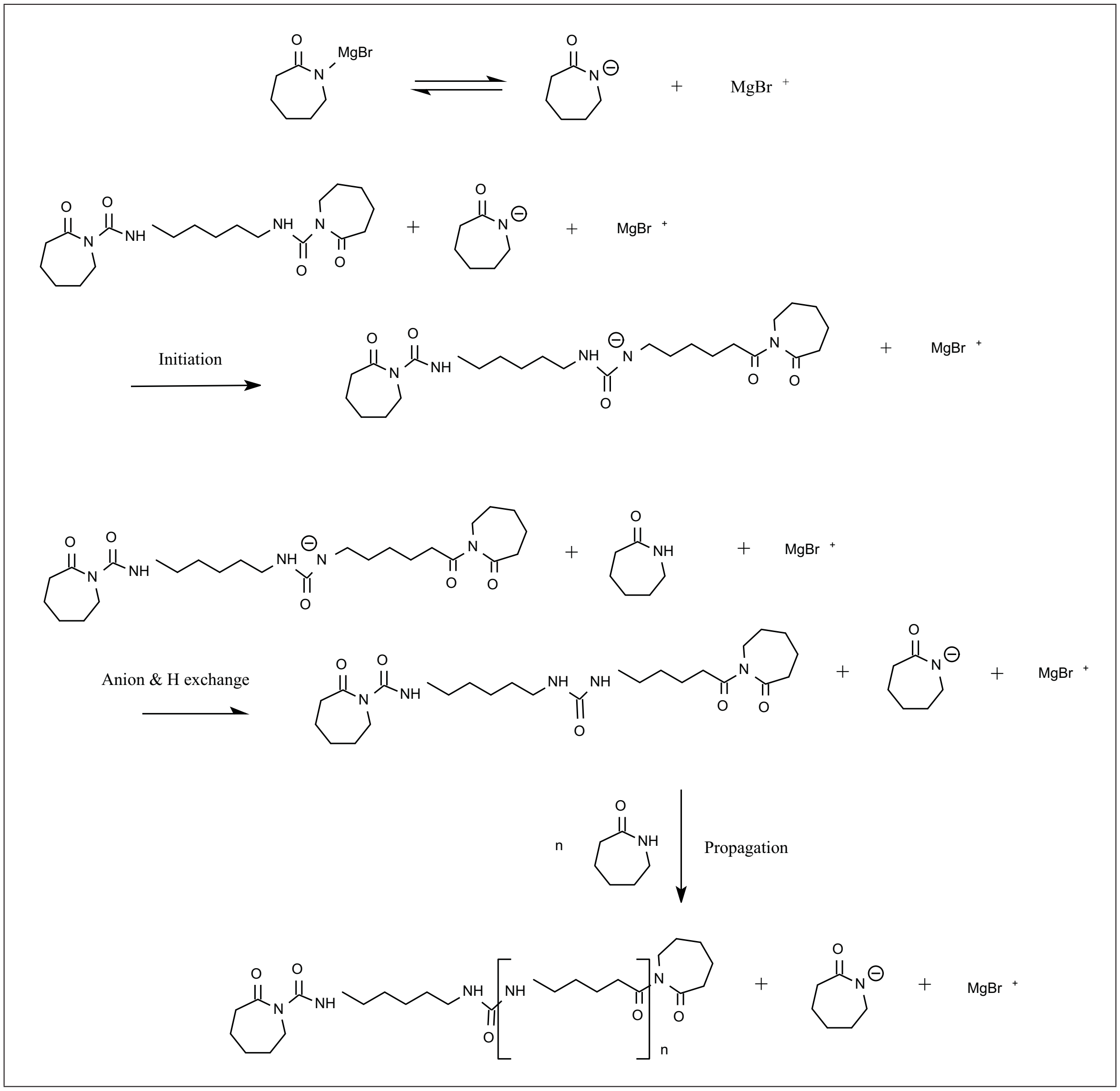

Figure 1.14 APA-6 polymerisation mechanisms, using HDCL as activator and MgBrCL as initiator.

which will translate into a potential temperature increase when adjusting the mould temperature and the chemical concentration [70].

Side reactions, like branching, can also occur while the polymerisation is on going, see figure 1.15. First, the activator has to de-block. It separates (splits) itself in two to create a monomer and an isocyanate end group molecule. De-blocking of the hexamethylene-1.6-dicarbamoylcaprolactam (HDCL) activator happens when the splitting temperature

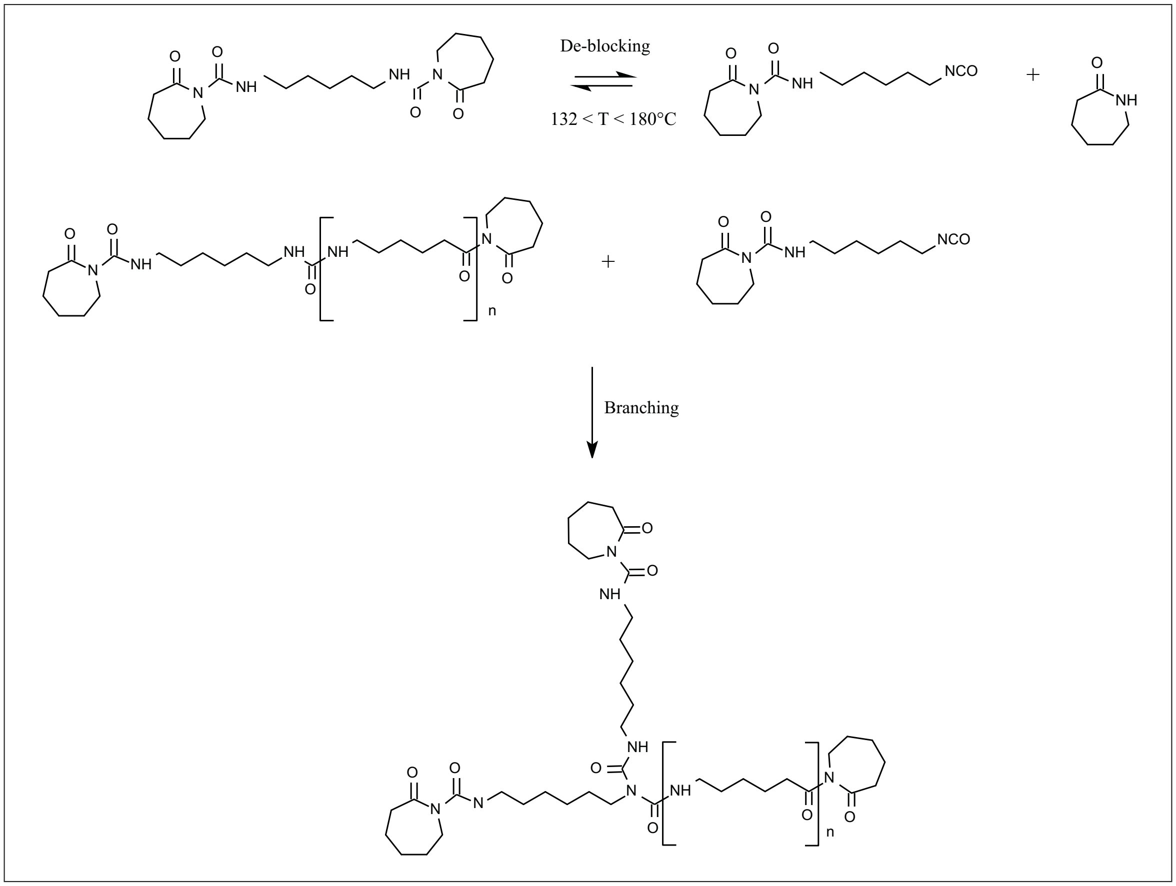

Figure 1.15 Branching mechanism.

is reached ($T_{de-block}$ = 132 – 180 ℃) [71, 72], otherwise HDCL is stable. Then, the isocyanate end group connects itself to a polymer chain on an imide functional group (— NH —) to create a branched polymer.

The reader is invited to read Roda's paper for more informations about the APA-6 polymerisation mechanism [73].

### 1.5.4 Activator functionality

The main function of an activator is to increase the polymerisation rate by adding growth centres, which are called either mono functional or multi-functional. The difference between these functionalities is the number of activation sites (the imide functional group) on the activator molecule. Each of these activation sites is a potential molecular chain start. Therefore, in an ideal polymerisation, the number of chains corresponds to the number of activation sites. A mono functional activator will have one activation site and gives one chain, while a difunctional activator, like HDCL, will be the starting point of two chains, shown on figure 1.13 b). Thus, difunctional activator enables a polymerisation that is two time faster than a mono functional activator for the same concentration [59]. Multi functional activators are expected to produce branched polymers. Hence, the weight-average molecular weights, $\bar{M}_w$, of APA-6 made with a difunctional activator is higher compared to those made with a mono functional activator because the polymer is branched [59, 74]. Also, the type and concentration of activator will affect the $X_c$ as will be explained in section 1.5.6.

### 1.5.5 Polymerisation time

A fast polymerisation is achieved by the synergy of both the initiator and activator. The initiator alone gives a slow polymerisation rate, while the activator alone has no reactivity under the same conditions. An activator added to an initiator solution accelerates the polymerisation rate and reduces the polymerisation temperature [60, 75]. Studies made with MgBrCL and NaCL initiators while using the same activator have showed that polymerisation time[5] is influenced by two parameters: the mould temperature and the initiator concentration [66, 76, 77]. The higher the polymerisation temperature, the lower the polymerisation time will be, *i.e.* the higher the polymerisation rate will be. At a fixed polymerisation temperature, the polymerisation time is governed by the initiator concentration, *e.g.* a high initiator concentration will result in a shorter polymerisation time. Consequently, the fastest reaction will be produced by the combination of both high temperature and high initiator concentration with a fixed difunctional activator concentration.

---

[5] The time required to complete their conversion from monomer to polymer.

### 1.5.6 APA-6 properties

The most important APA-6 properties are the degree of conversion (DOC) and degree of crystallinity ($X_c$). These will influence the overall performances of the given APA-6.

The DOC is the indicator that gives the amount of unreacted monomer still present in the polymer after its polymerisation. If the polymerisation is under control, then the DOC should be high ($\geq$ 95%). The unreacted monomer in the polymer acts as a plasticiser and has different consequences on properties. It decreases the polymer melting point because the monomer melting point is lower than its polymer. It also reduces the mechanical performance because its modulus and yield stress are lower than its polymer. Consequently, the DOC should always be maximised in the production of APA-6 and this is achieved by choosing the right combination of mould temperature and initiator/activator concentrations.

$X_c$ gives the information on the polymer crystal content after moulding. The crystallinity influences mechanical properties, such as modulus, tensile strength, toughness and fracture mode. Thus, like for all semi crystalline thermoplastics, a high crystalline content ($\geq$ 40 %) results in a higher modulus, tensile strength with a brittle planar fracture and low toughness [59,78,79]. Furthermore, the polymerisation temperature and the activator nature and concentration will have an influence on the degree of crystallinity and should therefore be adjusted. $X_c$ will be different for a mono or difunctional activator at a fixed polymerisation temperature. $X_c$ raises with monofunctionnal activator concentration increasement, while the reverse behaviour occurs when using a difunctional activator [74]. For this reason, it is more practical to adjust $X_c$ with the mould temperature (the $X_c$ will decrease with a high temperature and will raise with a lower temperature) [79].

### 1.5.7 APA-6 matrix for TP-VI

As mentioned earlier, research to develop a thermoplastic liquid moulding process for wind turbine blades using TP-VI of APA-6 is done at the DPCS group of the TU Delft in the Netherlands. Van Rijswijk *et al.* did adjustments on the APA-6 matrix used for the SRIM process to be adapted for the TP-VI. It was found that the combination of the HDCL/MgBrCL as activator/initiator was the most appropriate for mouldings large parts. This combination of activator and initiator permits longer mould filling times than other well known activator/initiator systems. Furthermore, the use of the HDCL has a better compatibility potential to bond with glass fibres [80]. Finally, the optimum mould temperature to maximise DOC and $X_c$ is around 140 – 150℃ [79].

This baseline resin formulation and process parameters will be used throughout this thesis as will be explained in section 2.2.1.

## 1.6 APA-6 composite

This section will review different topics related to the APA-6 composites. First, a part of its history, then a part on the adjustments made on the APA-6 system to be used for a composites instead of neat polymer. More specifically, the creation of the APA-6 composite interphase will be explained and different coupling agents will be shown. Finally, two infusion strategies are proposed to manufacture APA-6 composite laminates.

### 1.6.1 History

The oldest paper found about the use of APA-6 reinforced with long fibres is from 1969 [81]. It was to analysed different fibres with an APA-6 matrix moulded by what seems to be a monomer casting over pre-tensioned fibre mounted on a jig. Since then, APA-6 matrix has been used in many different moulding processes with different type of long fibres as reinforcement, *e.g.* compression moulding, VARTM, RIP and TP-Infusion with asbestos, aramid, carbon and glass fibres [82–90]. For any moulding and fibre reinforcement type, the goal is always the same; achieve the best interphase properties. Therefore, studies have been done on this subject since the beginning.

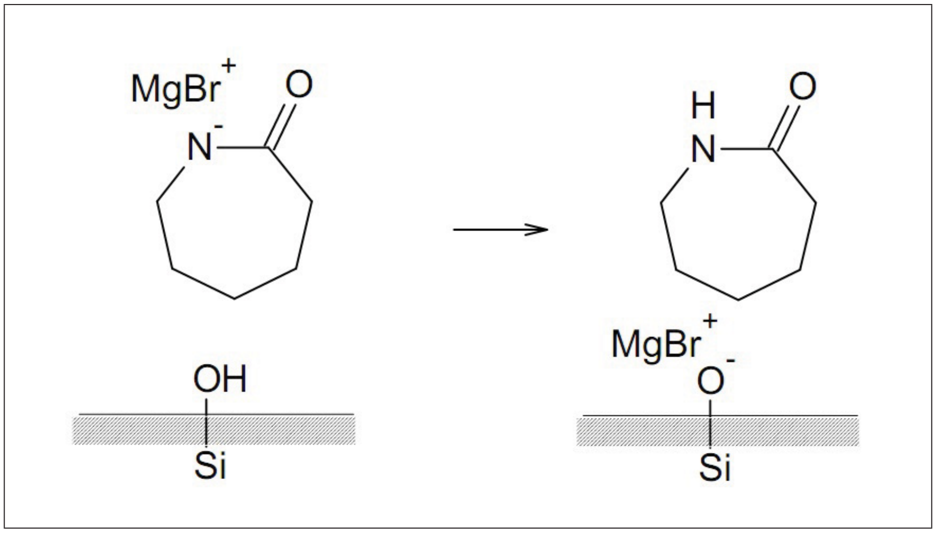

Figure 1.16 Deactivation of the anion by an untreated surface glass fibres. From [9]

### 1.6.2 Moulding adjustments of APA-6 composite

By adding glass fibres to the APA-6 matrix, some moulding adjustments have to be made because the glass fibres disturb chemical reactions. Since a composite has fibres in it ($\upsilon_f \approx 50\%$ for VI), less plastic (monomer moles) is involved in the polymerisation, thus the exothermic heat released by the reaction is reduced. Therefore, to compensate and to obtain the same matrix properties (DOC and $X_c$), the polymerisation temperature has to be raised by 10℃. Next, the humidity found on the glass fibres is responsible for the deactivation of the polymerisation reaction. Thus, the fibres should be dried before the infusion. Furthermore, the siloxyl groups of glass fibre surfaces also deactivates the polymerisation reaction by exchanging their hydrogen atom with the initiator transforming it into a regular $\varepsilon$-caprolactam, this is showed in figure 1.16. To maintain the catalyst system active, it is proposed to use only fibres coated with a coupling agent to mask the siloxyl groups [9].

### 1.6.3 Polyamide-6 composite interphase

The use of a coupling agent is also used to improve the interphase of a glass fibre composite or in others words the fibre to matrix bond, as described in section 1.1.3. The next sections will review the interphase of anionic and hydrolitic polyamide-6 composites.

#### 1.6.3.1 APA-6 composite interphase

The Monsanto Company claims, through patents, that APA-6 suitable silane based coupling agents are those which include these functional groups: the primary and secondary amino group, amido, isocyanate and epoxy [91] (see in table 1.5). Monsanto states that these are able to make chemical bonds from a polyamide and to an inorganic reinforcements, like glass fibres, without altering the polymerisation reaction. Monsanto's preferred coupling agents are primary amino and epoxy groups [92]. In their patent examples, the most used silane, and the one which enhanced the most the composite properties is the $\gamma$-aminopropyltriethoxysilane [84, 93, 94]. This silane is mixed directly in the monomer solution to mould an APA-6 composite [93]. The Monsanto hypothesis was confirmed later by Jenneskens *et al.* which established the adhesion of a polyamide-6 to a glass bead via the $-\mathrm{NH_2}$ group of a $\gamma$-aminopropyl silane coupling agent moulded by a hydrolysis method [95].

Other academical researches [85, 90, 103] have showed that aminosilane coupling agents improved the interphase of polyamides and glass. $\gamma$-aminopropyltriethoxysilane, shown in table 1.5, is again one of the most efficient so far [97,104,105]. The resulting composite has better tensile properties with pieces of APA-6 matrix still linked to fibres after fracture compared to an unfinished fibre surface reinforced composite. Van Rijswijk *et al.* have showed that the used of a de-blocking activator, like HDCL, eases bonding [96]. While the polymerisation and branching mechanisms are in progress, the APA-6 chains can connect to silane agents, via an urea link, if a lactam is de-blocked, as explained in section 1.5.3, see figure 1.17. Unfortunately, it seems to be impossible to maximise both

Table 1.5 Anionic polyamide-6 compatible coupling agent.

| **Organo-functional group** | **Name & formulas** | **CAS number** | **References** |
|---|---|---|---|
| Amine | $\gamma$-aminopropyltriethoxysilane<br>$NH_2(CH_2)_3Si(OC_2H_5)_3$ | 919-30-2 | [91, 92, 96] |
| Diamine | $N$-$\beta$-Aminoethyl-$\gamma$-aminopropyl-triethoxysilane<br>$NH_2(CH_2)_2NH(CH_2)_3Si(OC_2H_5)_3$ | 1760-24-3 | [92, 97–101] |
| Epoxy | $\gamma$-Glycidoxypropyltripropoxy-silane<br>$OCH_2CHCH_2O(CH_2)_3Si(OC_3H_7)_3$ | ? | [92] |
| Isocyanato | 3-isocyanatopropyltrimethoxy-silane<br>$OCN(CH)_3Si(OCH_3)_3$ | 15396-00-6 | [91] |
| ? | $N$-((3-triethoxysilylpropyl) (carbamoyl)) caprolactam<br>$(RO_3$-$Si$-$(CH_2)_n$-$NH$-$CO$-$N$-$(CH_2)_5$-$CO$ | ? | [102] |

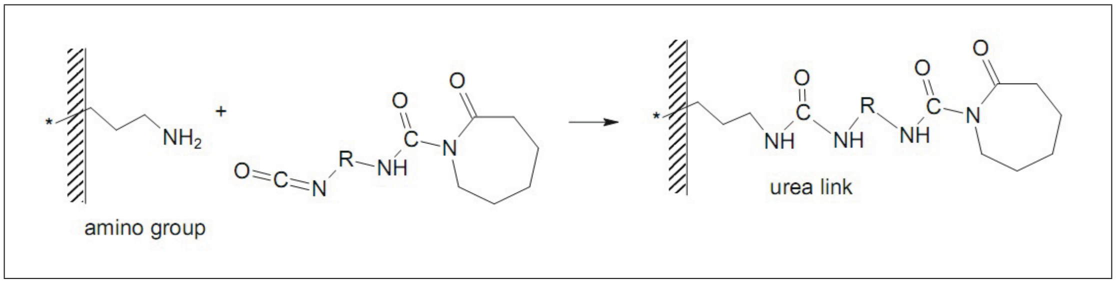

Figure 1.17 Fibre to matrix bond mechanism; Urea link via a de-blocked activator. From [96]

matrix properties (DOC and $X_c$) and the interphase. The ILSS is higher at 180°C while the matrix properties are higher at 160°C.

By using an unspecified compatible polyamides coupling agent, Bessell *et al.* produced a unidirectional glass fibre APA-6 composite polymerised at 180°C, which withstand 63 MPa of ILSS for a 40 $\upsilon_f$% [89]. This coupling agent seems to be effective because some small APA-6 parts were still attach to glass fibre after a tensile fracture. This is

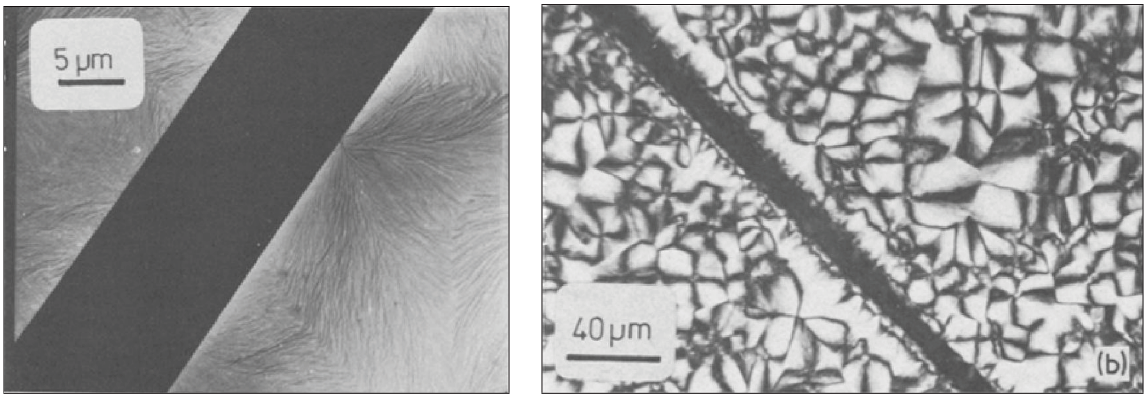

a) b)

Figure 1.18 Nucleation on glass fibre: a) transmission electron & b) optical micrographics.
From [88]

explained by a strong hydrogen bond between the fibre and reactive $-\mathrm{C}=\mathrm{O}$ and $-\mathrm{NH}$ groups of the polyamide [85]. The glass fibres nucleate a columnar structure (crystals) at the interphase, see figure 1.18. The crystallisation of APA-6 onto glass fibre surfaces is non-uniform and is influenced to some extent by the presence of the finish coating on the fibre surface. The crystal nucleation sites may be generated by the finish locally dissolved in the monomer solution [78].

With $\gamma$-Aminopropyltriethoxysilane, Joncas *et al.* and van Rijswijk *et al.* produced a 50 $\upsilon_f$% textile APA-6 composite showing ILSS between 70 & 75 MPa when polymerised at 180°C [96, 103].

Lechner *et al.* claim that a polyamide composite made with an amino silane is only suitable for an hydrolitic polymerisation. He argues that amino silane increases even more the hydrophilic behaviour of glass fibre. Consequently, the moisture alters the chemical reactions and results in an incomplete anionic polymerisation, thus a low DOC. The unreacted monomer creates hollow spaces around the fibres and thus reduces the mechanical properties of the composite. It is proposed to used two silane coupling agents on the glass fibers: the *N*-((3-triethoxysilylpropyl) (carbamoyl)) caprolactam, see table 1.5, and the bis-(3)triethoxysilylpropyl) amine to have a clean polymerisation between 100–150℃ [102]. It is interesting to notice that the *N*-((3-triethoxysilylpropyl) (carbamoyl)) caprolactam coupling agent contain a $\varepsilon$-caprolactam monomer like the HDCL activator used by van Rijswijk *et al.*. Therefore, this coupling agent is one of the most interesting to investigate as mentioned in recommendation 3.3.

#### 1.6.3.2 HPA-6 composite interphase

Plueddemann made studies on the interphase of glass fibres composites with silane coupling agents [22, 23]. Among these composites, the polyamide-6/glass fibres composite made by hydrolitic polymerisation have been tested with many different silane agents [101, 106, 107]. The silane agents in table 1.6 are all polyamide-6 compatible when used with a hydrolitic process, but it is difficult to tell which one enhances the most the interphase. Nevertheless, an interphase created by ionomer bonds is interesting to notice. It is a blend of adipic and isophtalic acids, with 1.6-hexane diamine and a diamine coupling agent mixed with $Mg^{2+}$ ions. This interphase is said to have outstanding strength retention after boiling in water compared to a state of the art coupling agent, *i.e.* the cationic styryl agent [101].

Cho *et al.* have compared four silane based coupling agents with different organo-functional groups on a glass fibre/polyamide-6 composite ($\upsilon_f = 0.4$) made by an hydrolitic polymerisation, compression moulding, to a commercial finish surface fibre composite. The melting temperature was 228℃ for 5 min, pressing at 6.89 MPa (1 000 psi) for 1.5 min and then naturally cooled down to ambient temperature. They have tested their laminates by the inter facial shear strength test (IFSS), ILSS and by fractography methods but DOC and $X_c$ of their laminates are unknown. Results showed that all the coupling agent tested promote better performances than the commercially finish fibre. The coupling agent with the chloropropyl organo-functional groups, see table 1.6, is the one which enhances the most the IFSS and ILSS. Furthermore, this chloropropyl coupling agent is the one which promotes the biggest amount of polymer pieces still attached to

Table 1.6 Polyamide-6 compatible coupling agent.

| Organo-functional group | Name & formulas | CAS number | References |
|---|---|---|---|
| Primary amine | $\gamma$-Aminopropyltriethoxysilane<br>$NH_2(CH_2)_3Si(OC_2H_5)_3$ | 919-30-2 | [96] |
| Diamine | $N$-$\beta$-Aminoethyl-$\gamma$-aminopropyl-triethoxysilane<br>$NH_2(CH_2)_2NH(CH_2)_3Si(OC_2H_5)_3$ | 1760-24-3 | [97–101] |
| Chloropropyl | $\gamma$-Chloropropyltrimethoxysilane<br>$Cl(CH_2)_3Si(OCH_3)_3$ | 2530-87-2 | [98–100] |
| Cationic styryl | $\gamma$-($N$-Styrylmethyl-$\beta$-aminoethyl-amino)-propyltrimethoxysilane hydrochloride<br>$CH_2{=}CHC_6H_4CH_2NHCH_2CH_2NH\text{-}(CH_2)_3Si(OCH_3)_3 \cdot HCL$ | 34937-00-3 | [100, 101, 107] |
| Epoxy | $\gamma$-Glycidoxypropyltrimethoxy-silane<br>$OCH_2CHCH_2O(CH_2)_3Si(OCH_3)_3$ | 2530-83-8 | [106] |
| Ionomer bonds | (0.9 mol ethylenediamine + 1.0 mol isophtalic acid) + (0.9 mol 1.6-hexane diamine + 1.0 mol adipic acid) + (0.4 $Mg^{2+}$) | ? | [101] |

the fibres after fracture [98, 99]. It is also noteworthy to know that the chloropropyl coupling agent promotes better performance than a diamine coupling agent very similar to the coupling agent used by van Rijswijk *et al.* Nevertheless, van Rijwijk's anionic ILSS are higher than Cho's hydrolitic ILSS.

### 1.6.4 TP-VI moulding strategies

For any moulding process, an effective strategy is required. Van Rijswijk *et al.* used two different strategies: non-isothermal and isothermal, for their TP-VI [96]. The non-isothermal process infuses of a relatively cold (110℃) monomer solution in a preheated preform (150 – 190℃). Therefore, through its flow, the monomer solution polymerisation rate increases as soon as it comes in contact with the hot surfaces of the mould. Consequently, the resulting composite is non-uniform, the ILSS and $X_c$ is different from the inlet to the outlet (in direction with the monomer flow), as showed on figure 1.19. To solve this problem the isothermal infusion was proposed, which consist of infusing the reactive mixture in a preform with the same temperature (110°C) as the monomer solution after which the fibres and the infused solution is heated to the polymerisation temperature (160 – 180°C). Thus, the monomer polymerised at the same time and should produce a uniform composite. The isothermal infusion attempted by van Rijswijk did improve the laminate uniformity (gradients were no longer visible) but not its properties as the ILSS tested were disappointingly low. This was attributed to the low mould temperature increasing rate (10°C/min) limited by the platen press, the heating equipment used at that time [96]. It is explained that with this heating rate it was impossible to un-block the activator before the polymerisation starts which reduces the urea links and ultimately gives poor fibre to matrix bond. A second reason for the bad laminate results is from some heat loss. The dimensions of the platen press are suspected to be too small to effectively cover the entire surface of the laminate to be infused.

As explained in section 1.6.3.1, a coupling agent is necessary to achieve a good interphase. Since the 8225 finish coupling agent is unknown, chapter 3 is an investigation on this coupling agent. It will evaluate its interphase and compare it to the interphase obtained with $\gamma$-Aminopropyltriethoxysilane in the previous work of van Rijswijk [96].

Furthermore, van Rijswijk did not succeed to enhance the uniformity of its APA-6 laminates while maintaining its (ILSS) properties. Therefore, chapter 5 is about the enhancement of the laminate uniformity and properties by the use of infusion strategies. To solve van Rijswijk too low temperature increasing rate problem, experiments in chapter 5 will be made with a higher temperature increasing rate made possible by the radiative set-up.

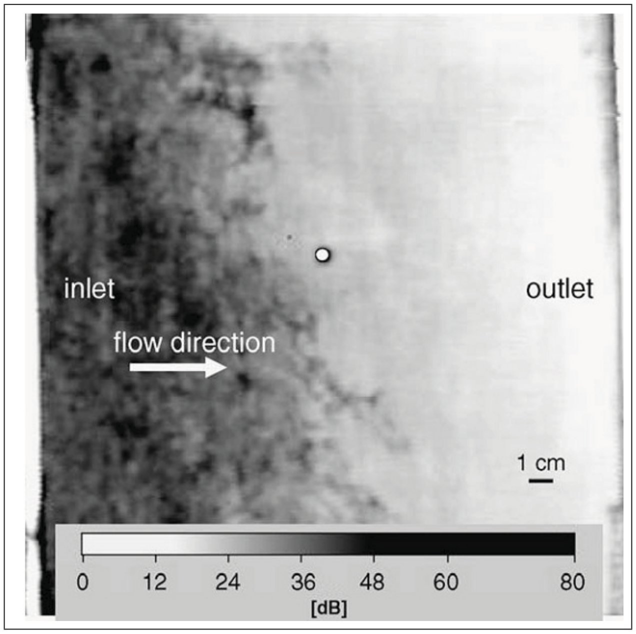

Figure 1.19 C-scan of a non-isothermal APA-6 composite laminate made by van Rijswijk. From [9]

# CHAPTER 2

# EXPERIMENTS

## 2.1 Introduction

This chapter is will describe the experimental materials, procedures and test methods used through the thesis.

## 2.2 Materials

The APA-6 matrix, the glass fabric, mould and consumable will be describe in the next section.

### 2.2.1 APA-6 matrix

The APA-6 monomer was an anionic polymerisation grade Caprolactam supplied by Brüggemann Chemical (Germany). This monomer was stored at room temperature in plastics jars with silica gel to maintain a dry atmosphere. Both activator and initiator were also supplied by Brüggemann Chemical in sealed polyethylene bags and then stored at room temperature in nitrogen atmosphere glass jars. The chemical formulation was equivalent to what Joncas [103] and van Rijswijk [9] used in previous work.

### 2.2.2 Glass fabric

An 8-harness satin weave E glass laminate fabric (SS 0303 050, 300 $g/m^2$) was supplied by Ten Cate Advanced Composites (Netherlands) with the proprietary fibre finish 8225. The 8225 finish coupling agent was unknown.

### 2.2.3 Mould and consumable

The mould was a 3 mm thick aluminium plate. The mould's exterior face was painted in black mat finish to maximise its emissivity. The release agent used was a NYRIM®

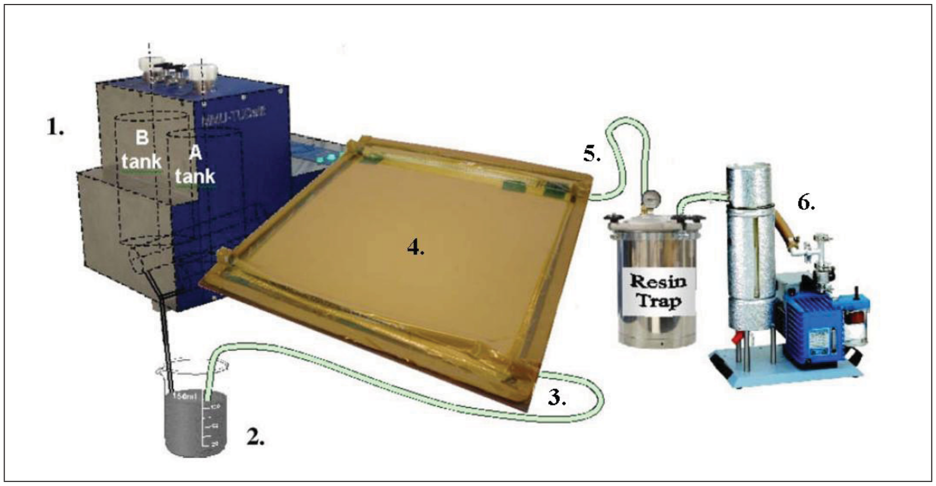

Figure 2.1 Process schematics: (1.) Mini Mixing Unit “MMU-TU Delft”, (2.) resin buffer vessel, (3.) inlet tube, (4.) mould and heating system, (5.) outlet tube and (6.) pressure control system. Adapted from [9]

mould sealer. The vacuum bag used was a UPILEX-R® 25 $\mu$m polyimide film sealed with tacky tape® from Schnee-Morehead, Inc (USA). The silicon rubber infusion tubes were from Rubber b.v. (Netherlands).

## 2.3 Processing

The laminate preparation, reactive mixture preparation, infusion generalities & strategies, control and monitoring will be covered in the next section.

### 2.3.1 Laminate preparation

The laminates were made of 12 balanced and symmetric cross-plies of 30 × 25 cm. For the laminates heated with the radiation method, temperature sensors were inserted in the middle of the lay-up. Sensors and control will be fully discussed in section 2.3.5. Then, as seen in figure 2.1, the inlet and outlet tubes were fixed on the top of the laminate edge. Afterwards, the vacuum bag was sealed with tacky tape directly over the top fibre glass layer without an infusion medium. Finally, the inlet and outlet tubes were connected through silicon rubber tubes to the buffer vessel and vacuum pump.

### 2.3.2 Reactive mixture preparation

The resin preparation was done with the Mini Mixing Unit (MMU) from Bronk Industrial b.v. (Netherlands) shown in figure 2.1. The activator tank (A), initiator tank (B) and buffer vessel were preheated to 110℃. The two tanks were filled with nitrogen at 20 kPa while a vacuum was maintained in the buffer vessel. The tanks were filled (with the monomer, activator and initiator), mixed and re-circulated prior to infusion in their respective tanks. At the start of the infusion process, the chemical solutions were mixed through a static mixer (1:1 ratio) into the buffer vessel. Finally, the mixed solution was degassed at 1 kPa (0.3 inHg) for five minutes.

### 2.3.3 Infusion generalities

While keeping the mould under vacuum, a nitrogen flow was circulated through the fibre glass bed for 5 minutes to remove any trace of moisture. Then, the infusion of the resin was performed at 25 kPa (7.38 inHg). From the buffer vessel (now open to the atmosphere) to the mould's inlet, the solution flowed through a silicon rubber tube kept at 110℃. When the laminate was fully impregnated and excess resin flowed through the outlet tube, the inlet was closed. Then, the polymerisation temperature was dwelled for 60 minutes. A complete illustration of this process is presented in figure 2.1.

### 2.3.4 Infusion strategies

All the strategies tested in this thesis (non-isothermal & double step) consist of infusing a monomer solution at 110℃ in the mould. The difference between these strategies was the mould temperature during the infusion and polymerisation periods.

#### Non-isothermal strategy

With the non-isothermal strategy, the mould temperature was the same for both periods. Prior to the infusion, the glass fibres were maintained under vacuum and pre-heated to the polymerisation temperature, as shown on figure 2.2 a). Since the resin temperature

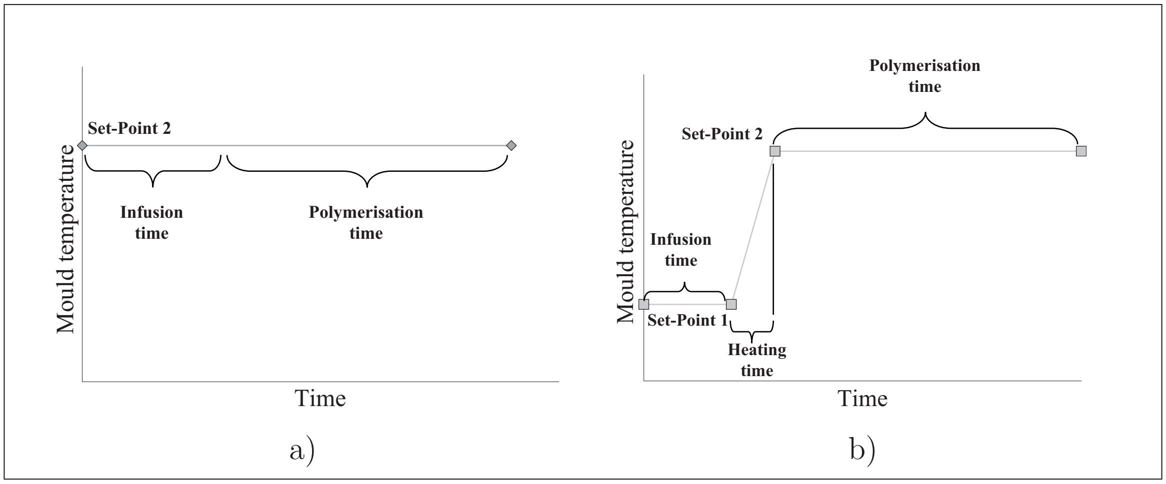

Figure 2.2 Infusion strategies. a) non-isothermal b) double step
set-point 1: infusion temperature &
set-point 2: polymerisation temperature.

is not identical as the mould temperature during the infusion, this strategy is considered non-isothermal.

**Double step strategy**

The double step infusion consists of infusing the laminate with an infusion temperature lower than the polymerisation temperature. Before the infusion, the fibres were maintained under vacuum and pre-heated to the infusion temperature (set-point 1 (SP1)). Then after closing the inlet, the infusion temperature (SP 1) was raised to the polymerisation temperature (SP 2), as shown on figure 2.2 b).

### 2.3.5 Control and monitoring

For the platen press set-up, two Eurotherm inc. (USA) thermal controllers regulated the temperature. The thermal controllers' thermocouples (TCs) were fixed to each hot plate of the platen press. Hence, the feedback temperature was gauged outside of the laminate.

For the radiative set-up, the temperature was regulated again by two Eurotherm inc. 2216e (USA) thermal controllers. The IR thermal controllers' TCs (3 & 4) were placed

Table 2.1 PID values

| **PID** | **Top** | **Bottom** |
|---|---|---|
| Pb | 54 | 52 |
| Ti | 551 | 548 |
| Td | 91 | 91 |
| Lcb | auto | |
| Hcb | | |

at mid thickness of the fibre bed, five centimetres from the edge as shown on figure 2.3. Therefore, the feedback temperature was gauged inside the laminate.

For the double step strategy, the controllers were adjusted with PID values to optimise delay time and temperature. These PID values, see table 2.1, were found by making an auto-run on both controllers with a staking of glass fibres under vacuum from 110℃ to 180℃. Also, the set point ramp rate (SPrr) was set to deliver the highest IR panel heating rate possible between the infusion (SP 1) and the polymerisation temperature (SP 2), see figure 2.2. SPrr set to 70℃/min gave the highest heating rate, 40℃/min.

For both strategies, three more K type TCs (1, 2 & 5) were used for monitoring the temperature profile in the laminates. These sensors were located on the right side of the laminate, close to the inlet (TC 1), at the centre (TC 2) and close to the outlet (TC 5), as shown on figure 2.3. Monitoring of the temperature profile was carried out from preheating to demoulding.

## 2.4 Tests methods

The degree of conversion, differential scanning calorimetry, short-beam strength, ultrasonic testing and microscopy tests will be describe in this section.

### 2.4.1 Degree of conversion test

The goal of the DOC test was to determine the weight of unreacted monomer still present in the TPC. Thin flakes were drilled off from the surface of the laminates and used as

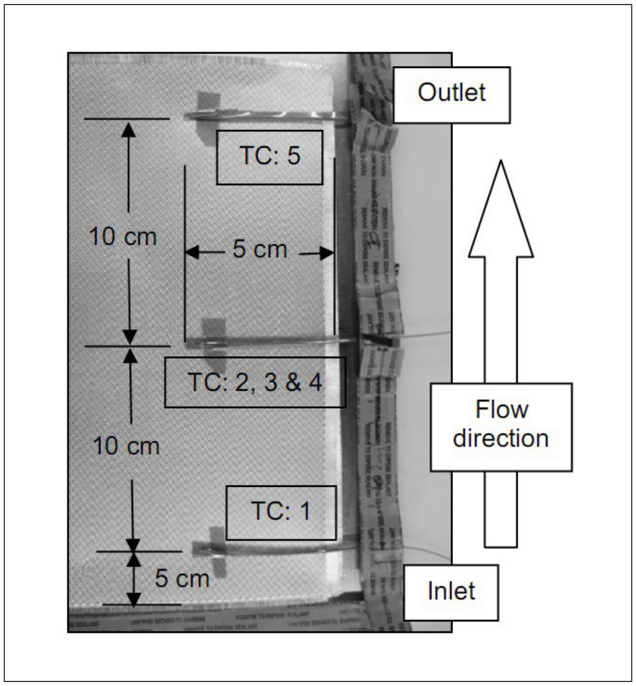

Figure 2.3 Thermocouples positions on laminate;
monitoring TC : 1, 2 & 5
control TC : 3 & 4.

samples. These samples were taken at 2.5 cm from both the resin inlet and the resin outlet. Then, the samples were brought back to their dry as moulded (DAM) state by maintaining them in a vacuum at 50°C for 48 hours. Next, the dried samples were weighed and their mass noted as $m_{tot}$. Afterwards, the samples were refluxed overnight in demineralised water to remove the water soluble monomer. By drying and weighing them again, the weight of loss monomer was known and noted as $m_{mon}$. After that, the polymer was burned off as recommended by ASTM D2584-02. The residual fibres were then cooled in a desiccator prior to weighing and their mass noted as $m_f$. The DOC can finally be determined from equation 2.1 [9, 52]. One sample of at least 0.4 g was drilled at each location.

$$\mathrm{DOC} = 1 - \frac{m_{mon}}{m_{tot} - m_f} \tag{2.1}$$

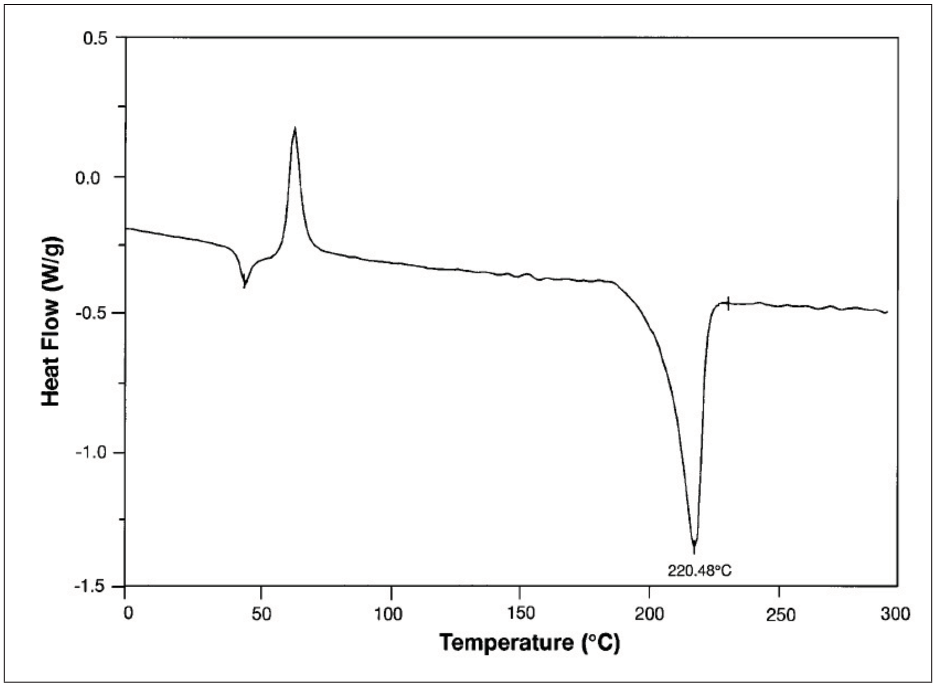

Figure 2.4 Typical DSC polyamide-6 curve. Adapted from [110]

### 2.4.2 Differential scanning calorimetry test

Since APA-6 is a semi-crystalline polymer, it has an amorphous and a crystalline phase. Therefore, to determine $X_c$ a Perkin Elmer DSC-7 machine was used. Circular samples were punched from the same location as the DOC samples. At least two specimens were tested by differential scanning calorimetry for each location. After DAM conditioning, the samples were weighed and their mass noted as $m_{tot}$. They were then kept at 25℃ for 2 minutes in the DSC-7 before being heated to 240℃ at a heating rate of 10℃/min. Afterwards, to obtain the fibre content correction, the matrix was burned off, the glass fibre mass was weighed and noted as $m_f$. The $X_c$ can then be calculated from equation 2.2 [9, 52], using the specimen melting enthalpy, $\Delta H_m$, and the fully crystalline polyamide-6 melting enthalpy, $\Delta H_{100}$, which is 188.4 J/g [108, 109]. The melt temperature ($T_m$) was also determined by the temperature on the abscissa corresponding to the maximum heat flow of the ordinate DSC curve. Per example, on figure 2.4 the melting temperature of the polyamide-6 sample is 220.48℃.

$$X_c = \left(\frac{\varDelta H_m}{\varDelta H_{100}}\right)\left(\frac{m_{tot}}{m_{tot} - m_f}\right)\left(\frac{1}{\mathrm{DOC}/100}\right) \tag{2.2}$$

### 2.4.3 Short-beam strength test

The short-beam strength (SBS), also known as the ILSS test, is a fast and reliable quality indicator of the overall performance of a fibre reinforced moulding process [111]. This test evaluates the synergy of the matrix, fibres and interphase. It was therefore used to benchmark the different heating set-ups as well as the infusion strategies. The test was performed according to ASTM D 2344 on a 20 kN Zwick-Roell machine. A minimum of five specimens were tested in DAM condition for both the laminate inlet and outlet regions. The samples dimension were 17 mm × 5.5 mm × 2.7 mm, which respected the standard. The ILSS was calculated from equation 2.3 in which $P_m$ was the maximum load achieved, $b$ was the width and $h$ the thickness of the sample. The thickness was measured with a ball-ball micrometre and the width with a vernier calliper.

$$F^{\mathrm{sbs}} = 0.75\left(\frac{P_m}{bh}\right) = \mathrm{ILSS} \tag{2.3}$$

### 2.4.4 Ultrasonic testing and microscopy

A high frequency ultrasonic C-scan was used to analyse the uniformity of the laminate. The data was obtained with a single through water transmitted signal of 10 MHz. The acquisition data grid was 0.5 mm and 1 mm in length and width. The images were analysed with the ALIS software with a dynamic range of 81.1 dB.

The C-scan results can quantify the uniformity of laminate by the ultrasonic signal attenuation. This signal was attenuated because of two reasons: by sound diffusion or sound absorption. The sound diffusion occurs when the signal reaches a defect in the material like a dislocation or a void. Consequently, the signal changes direction and will not be perceived by the receiving sensor. The signal absorption is proportional to the acoustic impedance of the material scanned. Each material absorbs the signal based on their density, thickness and on the wave propagation speed in the material.

Microscopy was used to confirm the either uniform or non-uniform laminate C-scan images. It was also used to investigate what could have caused the signal loss. The microscopies were done on a Leica DMLM optical microscope equipped with a CCD camera (projective 0.6 x), a 100 W illuminator power supply and the Qwin color software.

# CHAPTER 3

# ANALYSIS OF THE 8225 FINISH

## 3.1 Introduction

In 2008, the glass fibre supplier of the DPCS group stopped producing the finish 8207 which was containing the $\gamma$-Aminopropyltriethoxysilane used by van Rijswijk. Instead, the same supplier began to coat their glass fibres with the new finish 8225, which is said to be compatible with polyamides. Unfortunately, the coupling agent in the finish 8225 is unknown. Therefore, a benchmark study will be made to evaluate if the unknown coupling agent is compatible with the APA-6 system and if it is better or worst than its predecessor, the finish 8207.

Two laminates for each polymerisation temperature (160, 170 & 180℃) were infused with the non-isothermal strategy and the platen press using the same parameters as van Rijswijk (see figure 2.2 a)). Then, the laminates were tested to evaluated the DOC, $X_c$ and ILSS and compared to van Rijswijk's laminate results obtained with the 8207 finish [96].

## 3.2 Results

The results (DOC, $X_c$ and ILSS) of the composite made with the 8225 finish are presented in figure 3.1 next to the 8207 finish results of van Rijswijk [96].

## 3.3 Analysis

As mentioned in section 1.6.3.1, the glass fibre surface finish can influence the APA-6 composite since it modifies the laminates properties (DOC, $X_c$ and ILSS).

Figure 3.1 shows that all property values (DOC, $X_c$ and ILSS) are modified but their trend stays the same, except for the DOC. Indeed, the DOCs made with the 8225 finish

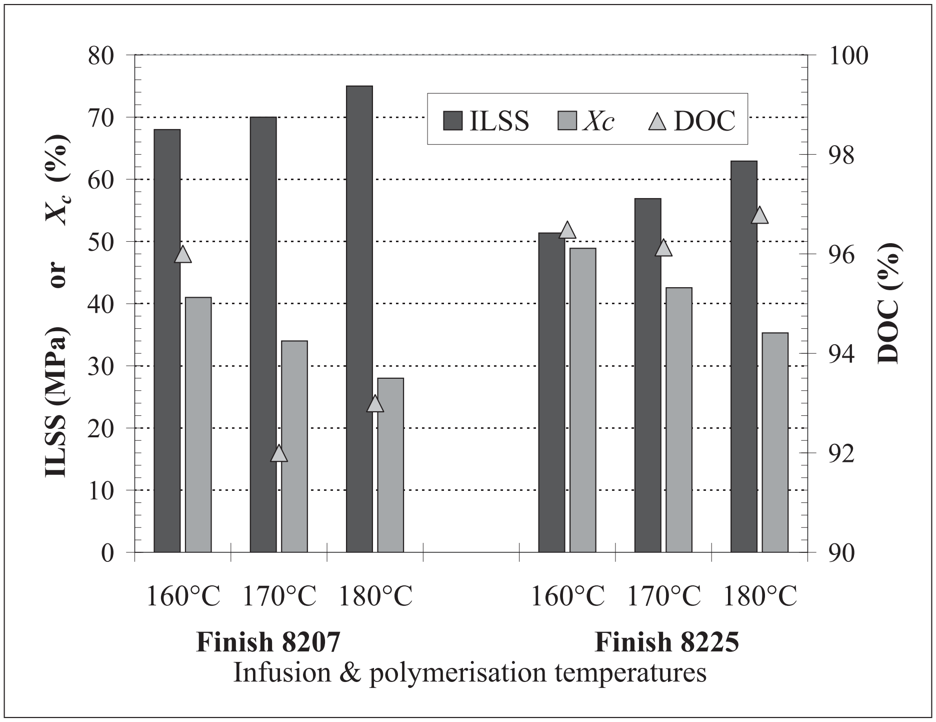

Figure 3.1 Result of the finish 8225.

are higher and more stable, around 96.5%, compared to those infused with the 8207, meaning that the polymerisation process with the finish 8225 is more under control.

The ILSS using the 8225 finish are lower but the $X_c$ are higher compared the 8207 finish. The difference in ILSS and $X_c$ between the two finishes could be explained by the coupling agent contained in each finish. It is believed that the use of different coupling agent influences the crystals growth and indirectly the ILSS since it acts as a chain growth nucleation site. Thus, the interphase morphology, the nature and the amount of crystals, depend on the coupling agent and on the moulding temperature. For the laminate made with the 8207 finish, as explained in section 1.6.3.1, the deblocked activator (HDCL) will link itself via an urea link from its isocyanate group (—NCO —) with the amino group (—NH —) of the silane molecule $\gamma$-aminopropyltriethoxysilane contained in the 8207 finish. Unfortunately, the coupling agent in the 8225 finish is unknown; therefore, the organofunctional group of the coupling agent is also unknown. Consequently, it was not possible to draw any conclusions on the interphase creation mechanisms. It would be essential to know which coupling agent is used in the 8225 finish to understand its effect on the chemical reactions.

## 3.4 Conclusion

In conclusion, two fibre glass finishes have been infused with the non-isothermal strategy. These laminates have been tested to measure their DOC, $X_c$ and ILSS. The 8225 finish is not better or worst than the 8207, but it is certainly compatible with an APA-6 system. The 8225 finish offers higher DOC & $X_c$ but lower ILSS when compared to the 8207 finish. DOCs higher than 96% mean the polymerisation is under control while high $X_c$ means a more rigid composite with a lower water uptake potential since water cannot enter the crystal morphology. A lower ILSS made with the 8225 finish means the overall performance of the composite is less than an APA-6 composite made with the 8207 finish. The reason why the 8225 finish behaves this way is unknown since its coupling agent is also unknown.

# CHAPTER 4

# MODIFICATION OF THE HEATING EQUIPMENTS

## 4.1 Introduction

As discussed in section 1.6.4, one of the reasons van Rijswijk *et al.* were unable to produce a uniform composite while maintaining its properties was the dimensions of the platen press which are suspected to be too small to effectively cover the entire surface of the mould, see figure 4.1 a). Thus, a new radiative set-up made of infra-red lights is tried, see figure 4.1 b). This radiative set-up covers the entire surface of the mould. Again, a benchmark study will be made to compare the two set-ups and to identify the one which produces the laminates with the highest DOC, $X_c$ and ILSS. The laminates of this study will be infused with the non-isothermal strategy, as explain in section 2.3.4.

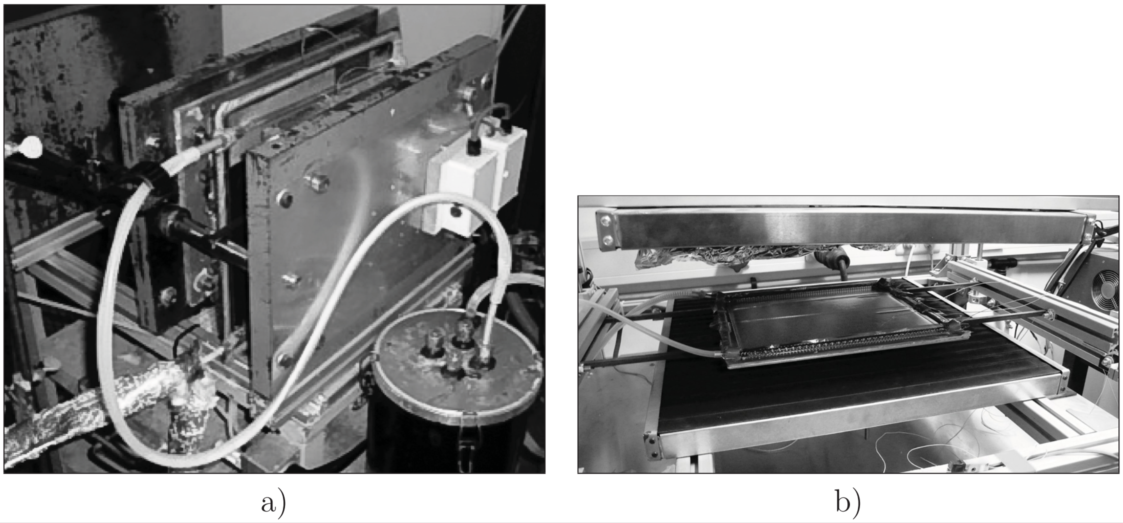

a) b)

Figure 4.1 Heating equipments: a) platen press, b) infra-red panels

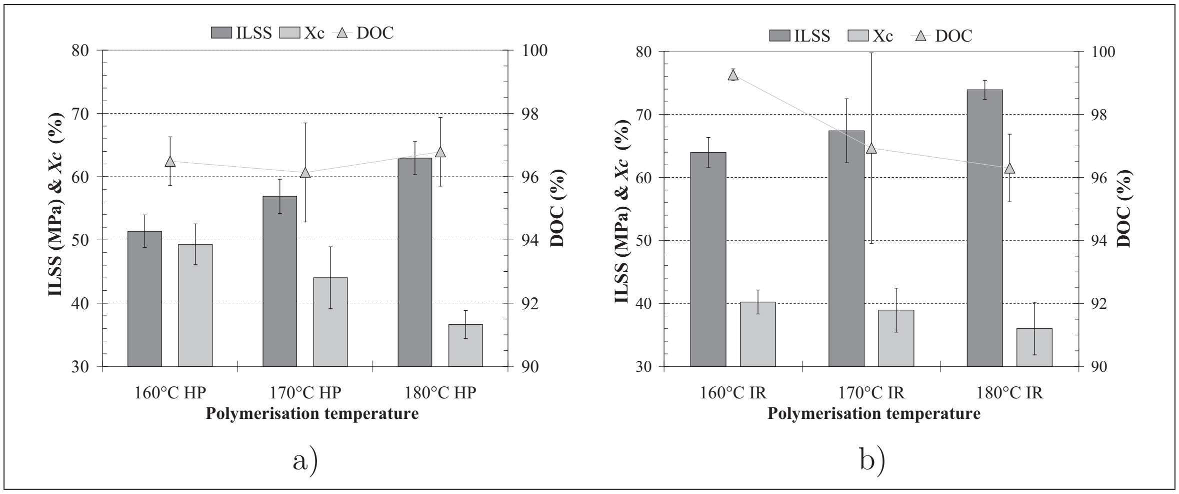

Figure 4.2 ILSS, $X_c$ and DOC of the laminates.
a) produced by the platen press. b) produced by the IR panels.
The error bars show the standard deviation.

## 4.2 Difference in heating set-ups

For the platen press, the mould was inserted between two, 25 cm × 25 cm, vertical hot plates. The heating plates were put in contact with both of the mould's faces to ensure conduction heating but precautions were taken to ensure that the contact pressure did not hinder the resin flow. For the IR panel set-up, the mould was inserted between two, 50 cm × 50 cm, horizontal IR panels. Both the bottom and top of the mould were separated by 3 cm from IR panels.

## 4.3 Results

In this section, the comparison of the two heating mould methods will be done by comparing figure 4.2 a) with b) and also with table 4.1. These graphs show the averages of inlet and outlet values of the ILSS, $X_c$ and DOC results for both heating set-ups.

Table 4.1 Results of the mould heating methods evaluation: ILSS, $X_c$, $T_m$ and DOC.[a]

| **Set-up** | **Infusion temperatures** | **ILSS** (MPa) | | $X_c$ (%) | | $T_m$ (°C) | | **DOC** (%) | |
|---|---|---|---|---|---|---|---|---|---|
| | | $\bar{X}$ | $\sigma$ | $\bar{X}$ | $\sigma$ | $\bar{X}$ | $\sigma$ | $\bar{X}$ | $\sigma$ |
| Platen press | 160°C | 51.4 | 2.6 | 49.3 | 3.2 | 224.46 | 2.22 | 96.5 | 0.8 |
| | 170°C | 56.9 | 2.7 | 44.0 | 4.9 | 221.09 | 1.67 | 96.1 | 1.6 |
| | 180°C | 62.9 | 2.6 | 36.6 | 2.2 | 220.14 | 1.49 | 96.8 | 1.1 |
| Radiative | 160°C | 63.9 | 2.4 | 40.2 | 1.9 | 219.38 | 2.43 | 99.3 | 0.2 |
| | 170°C | 67.4 | 5.1 | 39.0 | 3.5 | 218.13 | 2.22 | 96.9 | 3.0 |
| | 180°C | 73.9 | 1.5 | 36.0 | 4.9 | 216.08 | 2.56 | 96.3 | 1.1 |

---

[a] $\bar{X}$: average & $\sigma$: standard deviation

### 4.3.1 ILSS results

On a global perspective, the ILSS is maximised at a mould polymerisation temperature of 180°C. This statement is valid for both heating set-ups and was also observed by van Rijswijk [9].

However, on a comparative basis, the ILSS differences for the different heating set-ups are high. The ILSS obtained for laminates made with the IR set-up are all at least 17% higher than the ILSS values found for laminates produce with the conduction heating method.

### 4.3.2 DSC results

As observed in figure 4.2 a), the $X_c$ of laminates produced with the platen press are decreasing as the mould polymerisation temperature is increased. This behaviour was also reported by van Rijswijk [9] and Teuwen [8]. The $X_c$ of laminates produced with IR panels decreases at a rate much lower than the laminates produced with the platen press. Thus, the $X_c$ of the laminates made with the radiative set-up seems to be less sensitive to the mould polymerisation temperature. The radiative set-up yields lower $X_c$ averages for the laminates produced at a mould polymerisation temperature of 160°C and 170°C

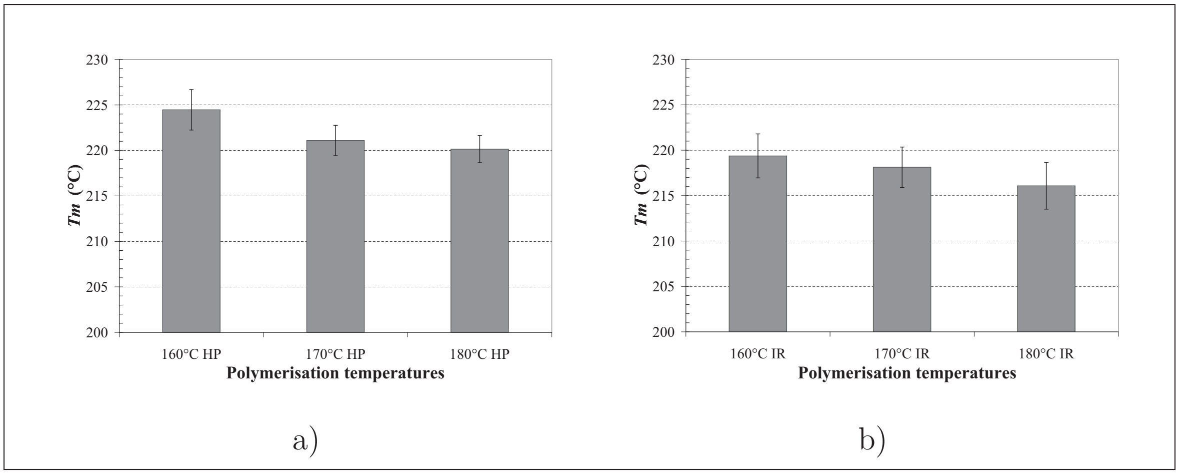

Figure 4.3 $T_m$ of the laminates.
a) produced by the platen press. b) produced by the IR panels.
The error bars show the standard deviation.

when compared to the platen press set-up. However at 180°C, the $X_c$ are the same for both set-ups.

The same trend happens to the $T_m$. It decreases with a higher polymerisation temperature, see figure 4.3. This is normal since a high $X_c$ will promote a high $T_m$. Also, when comparing both set-ups, the $T_m$ of the laminates made with the IR set-up are all lower than the platen press laminates. This correlates well with the previous $X_c$ results.

### 4.3.3 DOC results

Theoretically, it is impossible to achieve a complete monomer to polymer conversion. As explained by Rijswijk [52], Kohan [112] and Aharoni [113], some residual monomer will always remain present after production of APA-6. Since the unreacted monomer does not have any load carrying capabilities, it is critical to maximize the DOC.

The DOC results, presented in figure 4.2, show that both heating methods produce laminates with similar DOC. All DOC results are above 96 % which is acceptable for both heating methods and is comparable to values obtained by van Rijswijk [9]. However, the DOC standard deviation of the laminate produced with IR panels at 170°C is too high to state any behaviour related to temperature. Consequently, the DOC results cannot be used to conclude on the heating method used versus laminate uniformity.

## 4.4 Analysis

The ILSS increase and the $X_c$ decrease for laminates produced with IR panels compared to laminates processed with the platen press are believed to be due to heat loss.

The way heat is provided to the laminate is suspected to influence the results. The main difference between the two methods lies in the fact that the heating plates only cover the laminate surface (the edges of the mould are outside the heating plates) while the IR panels cover the whole mould. Since the heating plates are not heating the edges of the mould, they have a tendency to act as a heat sink and thus reduce the temperature at the edge of the laminate.

Furthermore, the radiative heat transfer can transmit electromagnetic waves through a semitransparent medium like the polyimide vacuum bag wherein used. When a semitransparent solid is irradiated, portions of this irradiation are reflected, absorbed and transmitted. Thus, the glass fibres under the vacuum bag are also heated by transmitted electromagnetic waves from the IR panel. Since the absorptance of the polyamide vacuum bag is 0.32 [114] there is either reflected and/or transmitted waves potential. Tsilingiris [115] reported that Kapton®, a polyimide film, can transmit electromagnetic waves over a wave length range of 2 – 5.5 $\mu$m, which is within the typical peak energy wavelength of the IR panels used in this set-up, 3 – 3.5 $\mu$m [116]. Moreover, Tsilingiris also showed that a Kapton® film of 100 $\mu$m can transmit 16 % of the received radiation at 180°C. He also showed that radiation transmission increases as the film thickness decreases. Therefore, the polyimide vacuum bag used (25 $\mu$m) is expected to transmit even more than Tsilingiris's film. The IR set-up seems to indirectly enhance the laminates ILSS and $X_c$ by promoting a good heat transfert.

## 4.5 Conclusion

It could be concluded that the material property averages were in general improved with the IR panel set-up. More specifically, laminates produced at 180℃ showed the best properties. This combination of heating method and polymerisation temperature led the laminate to reach the highest ILSS mainly because of the more uniform heat transfer.

# CHAPTER 5

# INFUSION STRATEGIES

## 5.1 Introduction

Since the results presented in chapter 4 showed that laminates infused at 180℃ with the radiative set-up yielded the best laminates properties, this set-up and polymerisation temperature was selected for a second set of experiments. This radiative set-up has higher heating rate (40℃/min maximum) than the platen press, thus it should be able to un-block the activator before the polymerisation starts. Consequently, give good fibre to matrix bond. The objective of this second set of experiments was to improve the uniformity of laminate properties by using the double step processing strategy. As explained in section 2.3.4, this strategy involved different infusion temperatures (110℃, 130℃ & 150℃). These laminates will be analysed by comparing their DOC, $X_c$, $T_m$, ILSS, C-scan and micrographics

## 5.2 Results

The results (ILSS, $X_c$, $T_m$ and DOC) of laminates made with the double temperature step strategy are presented in figure 5.1 and table 5.1.

Table 5.1 Double step strategy results, ILSS, $X_c$ & DOC.

| **Infusion temperatures** | **ILSS** (MPa) | | $X_c$ (%) | | $T_m$ (℃) | | **DOC** (%) | |
|---|---|---|---|---|---|---|---|---|
| | $\bar{X}$ | $\sigma$ | $\bar{X}$ | $\sigma$ | $\bar{X}$ | $\sigma$ | $\bar{X}$ | $\sigma$ |
| 110℃ | 67.9 | 1.1 | 39.1 | 3.7 | 217.26 | 0.61 | 95.9 | 0.4 |
| 130℃ | 70.4 | 1.0 | 37.8 | 2.2 | 218.28 | 0.88 | 95.7 | 0.6 |
| 150℃ | 70.9 | 1.6 | 40.0 | 0.7 | 219.94 | 1.48 | 95.7 | 1.2 |
| 180℃ | 73.3 | 1.7 | 35.7 | 4.1 | 216.08 | 2.56 | 96.3 | 1.1 |

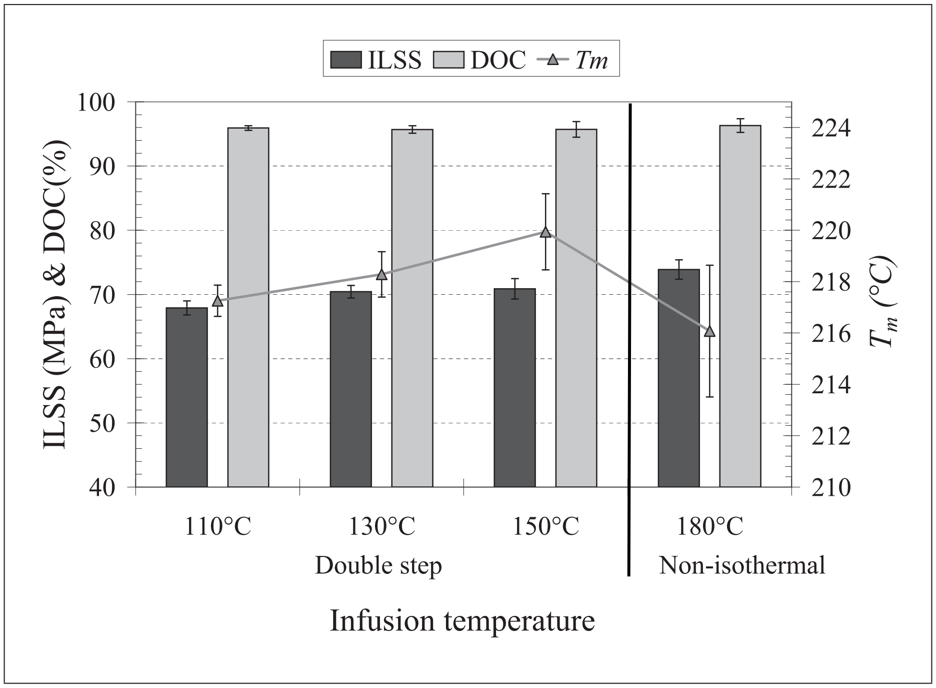

Figure 5.1 Double step ILSS, $T_m$ & DOC results.
The error bars show the standard deviation.

### 5.2.1 DSC results

The $X_c$ of all the laminates produced are around the same average and have relatively large standard deviation except for the one infused at 150℃ which shows the highest $X_c$, 39.95%, with the smallest standard deviation, 0.72%. Consequently by these results, this double step infusion temperature, 150℃, is the one which would enhances the most uniform $X_c$.

However, the relation between the $X_c$ and $T_m$ is not respected as it was the case for the past study presented in section 4.3.2, see figure 5.2. The $T_m$ should follow the $X_c$ trends, average and standard deviation.

The $T_m$ increases with the infusion temperature to a maximum of 219.94℃ at an infusion temperature of 150℃, see figure 5.2. Then at 180℃, the $T_m$ drops lower than at 110℃. The $T_m$ standard deviation at 110℃ is the lowest, 0.61℃, and increases with the infusion temperature raise to a maximum at 180℃, 2.56℃. Based on the $T_m$ standard deviation,

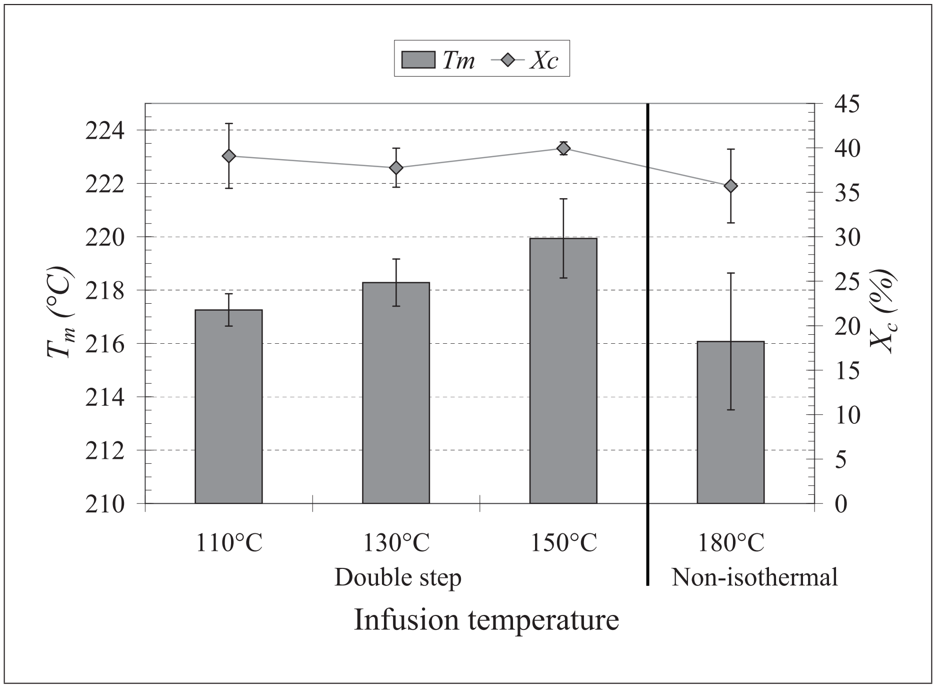

Figure 5.2 Double step laminates $T_m$ & $X_c$. The error bars show the standard deviation.

the double step strategy produces more uniform laminates at all infusion temperatures compared to the laminates made with the non-isothermal strategy. Also, the infusion temperature of 110°C would be the one which enhances the most uniform $T_m$.

### 5.2.2 ILSS results

Before analysing the ILSS results, it is important to notice that one of each laminate infused at 110°C and 130°C have voids at their outlet location (see blue areas, around 48 dB, on figure 5.3). Voids alter the ILSS [117–119], therefore these voided laminates were excluded from the ILSS results of figure 5.1 and table 5.1. Unfortunately, the ILSS analysis will only be based on the results of one laminate for each infusion temperature.

The ILSS increases as the infusion temperature increases to a maximum of 73.89 MPa at 180°C. However, the standard deviation of the laminates processed at 180°C is the second highest with 1.51 MPa. The 110°C and 130°C ILSS standard deviation, 1.10 & 0.97 MPa respectively, are lower that those produced at 150°C and 180°C. This means the laminates produced with the double step strategy at 110°C and 130°C have more uniform ILSS compared to those from the non-isothermal strategy.

### 5.2.3 DOC results

The DOC results are once again not helping to select the best infusion temperature since they show similar average values, 96%. Also, their standard deviation bars are all overlapped. Therefore, any of these infusion temperatures yielded acceptable and similar DOC.

### 5.2.4 Ultrasonic testing and micrographics results

The laminates were also observed by means of ultrasonic testing (C-scan) and microscopy to analyse the quality of the laminates. The images shown in figure 5.3 represent the signal loss by either defects like voids, density or thickness variations generated by the different matrix constituents (crystal phases & amorphous phase) and $\upsilon_f$. To know if the signal loss was related to voids, microscopy tests were performed.

From figure 5.3, the main signal loss seems to be located at the outlet of laminates infused at 110°C, 130°C and 180°C. Taking into account the micrographics shown in figure 5.4, the signal loss at the outlet of the laminate infused at 110°C and 130°C is most probably caused by the presence of voids. On the other hand, the micrographics for an infusion temperature of 150°C (or green areas of $\approx$ 24 dB), shown in figure 5.4, confirm that laminates are free of voids. Nevertheless, at least one of the laminates at 110°C, 130°C and 150°C show no signal loss compared to the non-isothermal laminate infused at 180°C and to van Rijswijk's non-isothermal laminate, see figure 1.19.

The average and standard deviation of signal loss of areas without voids (void less laminates) are presented in table 5.2. The laminates infused at 130°C show the lowest signal loss standard deviation of 0.54 dB. C-scan results suggests that the laminates infused

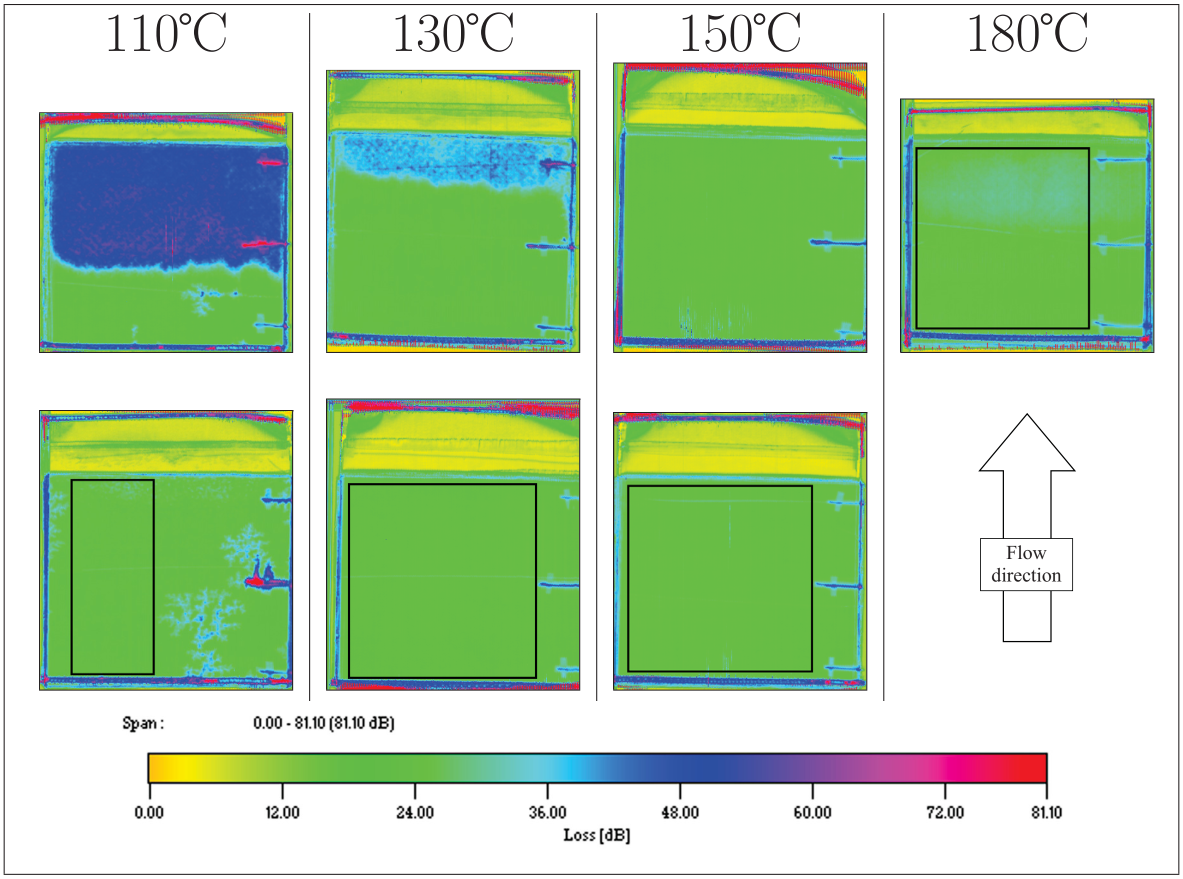

Figure 5.3 C-scan images of laminates done by the double step strategy. The rectangles show where the data samples are taken for table 5.2.

Table 5.2 Average & standard deviation of the C-scan signal loss on void less areas.

| **Infusion temperatures** | **Signal loss** (dB) | |
|---|---|---|
| | **Average** | **Standard deviation** |
| 110°C | 23.93 | 0.98 |
| 130°C | 23.91 | 0.54 |
| 150°C | 24.57 | 0.68 |
| 180°C | 26.17 | 1.57 |

with the double step strategy are more uniform than those made with the non-isothermal strategy. Furthermore, the laminates infused at 130°C are more uniform.

| **Infusion temperatures** | **Inlet** | **Outlet** |
|---|---|---|
| 110℃ 10X optic zoom | 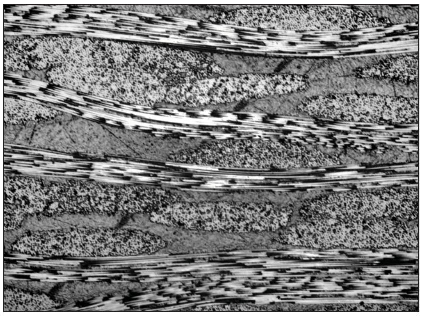 | 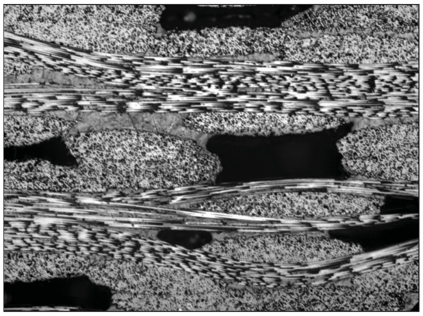 |
| 150℃ 10X optic zoom | 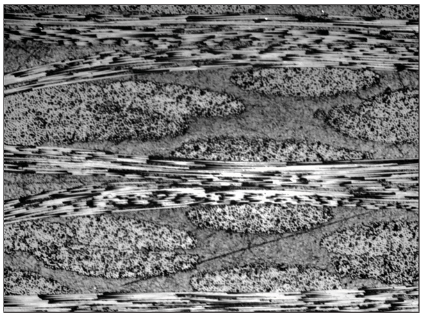 | 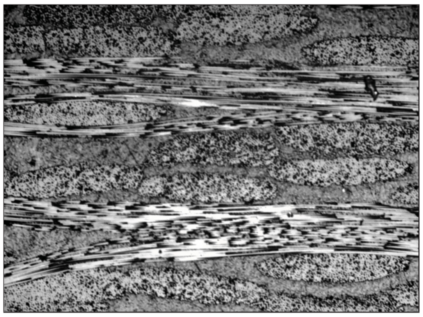 |
| 150℃ 50X optic zoom | 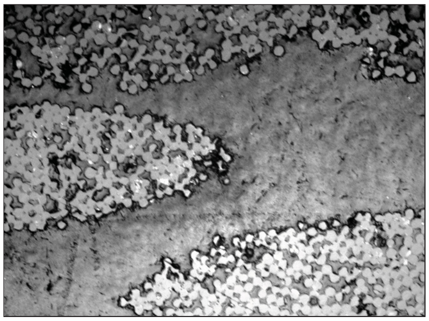 | |

Figure 5.4 Corresponding C-scan laminate micrographics.

## 5.3 Analysis

This section analyzes three behaviours of the laminates. It demonstrates how the two strategies influence the uniformity of the laminates by the means of the processing temperature profiles. Then, it explains the reason why a higher melt temperature occurs at 150℃ and why the ILSS of the non-isothermal strategy at 180℃ is higher than those of the double step.

### 5.3.1 Processing temperature profiles

From the processing temperature profiles, shown in figure 5.5, it is possible to see that the elapsed time & temperature between the first (at the outlet location) and the last (at the inlet location) exothermic peak differs depending on the infusion temperature used. Table 5.3 presents these elapsed time & temperatures. The double step elapsed time is at minimum half the time of the non-isothermal strategy elapsed time. Also, the difference in temperature of the exothermic peaks ($\mathit{\Delta} T_{peak}$) for the double step processing are less than for non-isothermal processing. Consequently, the $T_m$ and signal loss standard deviations of the double step strategy are lower than those from the isothermal strategy. Therefore, it is logical to believe that the closer the exothermic peaks are (in time and temperature), the more uniform the laminate will be.

### 5.3.2 Higher melt temperature at 150℃

The reason why $T_m$ is higher at 150℃ can be explained by the combination of two process temperatures, the HDCL de-blocking temperature and the APA-6 crystallisation temperature. As seen in section 1.5.3, the HDCL de-blocks at a temperature range of 132℃ to 180℃ and the APA-6 crystallisation temperature in a range of 90℃ to 185℃.

During infusion, the matrix benefits from the mould temperature set at 150℃, because it has more time to de-block and connect itself to the proprietary 8225 finish glass fibre coupling agent before the polymerisation rate increases. At 110℃ and 130℃, the matrix has less time to de-block since it is infused below its de-blocking temperature and then heats up to the polymerisation temperature, 180℃. At 150℃, this temperature is right in the de-blocking temperature range of the HDCL, therefore the de-blocking time is longer than when infusing at 110℃ and 130℃.

Furthermore, the $T_m$ is maximum at 150℃ because laminates were infused close to the optimum neat resin crystal formation rate of 138℃ [67]. While and after the HDCL de-blocks, a low rate polymerisation with an optimum crystallisation rate occurs until

Table 5.3 Elapsed time & temperatures between the first and last exothermic peaks

| **Strategies** | **Infusion temperatures** (°C) | **Elapsed time** | $\Delta T_{peak}$ (°C) | $T_m$ **standard deviation** (°C) |
|---|---|---|---|---|
| Non-isothermal | 160 | 7 min 0 s | 1.41 | 2.43 |
| | 170 | 4 min 54 s | 7.34 | 2.22 |
| | 180 | 4 min 40 s | 16.78 | 2.56 |
| Double step | 110 | 1 min 40 s | 5.77 | 0.61 |
| | 130 | 1 min 50 s | 4.52 | 0.88 |
| | 150 | 2 min 25 s | 4.10 | 1.48 |

the mould temperature increases to 180°C. Then, the polymerisation rate increases while the crystallisation rate slows down. Therefore, the amount of crystals is maximized by an infusion temperature of 150°C. Consequently, the laminates done with the double step strategy at 150°C present the highest $T_m$ of the group.

### 5.3.3 The high non-isothermal ILSS at 180°C

Figure 5.5 could explain why the non-isothermal ILSS at 180°C is higher than the ILSS of laminates infused with the double step strategy, see figure 5.1 or table 5.1. The 180°C non-isothermal exothermic processing peak went up to 196.46°C compared to ≈ 182°C for the double step infusion strategy. This increase in temperature, 14°C, affects the polymerisation and crystallisation processes and consequently the ILSS of the produced laminate.

## 5.4 Conclusion

Results have shown that the double step infusion strategy produces more uniform laminates compared to the non-isothermal strategy. For all the infusion temperatures tested, DOC results proved that the polymerisation is under control. The ILSS and $T_m$ standard deviation were the lowest at 130°C and 110°C respectively. The uniformity and quality of the laminate was also confirmed by ultrasonic testing and microscopy. The lowest signal loss average and standard deviation was found at 130℃. The infusion temperature which promotes the most uniform laminates is not easily determined, but it is most probably between 110℃ and 130℃. From the processing temperature profiles, the improvement in laminate properties uniformity could be explained by the fact that the polymerisation and crystallisation exothermic peaks occurs almost simultaneously for the double step strategy while the exothermic peaks can occurs 7 minutes apart between the inlet and outlet for the non-isothermal processing strategy.

| **Non-isothermal** | **Double step** |
|---|---|
| 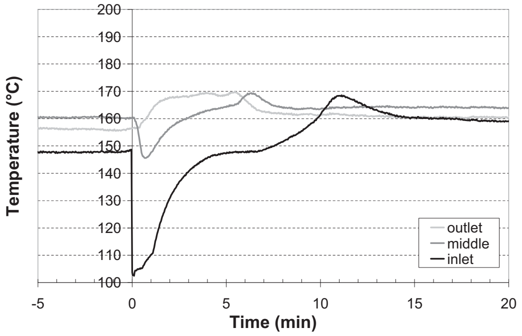 <br>160°C | 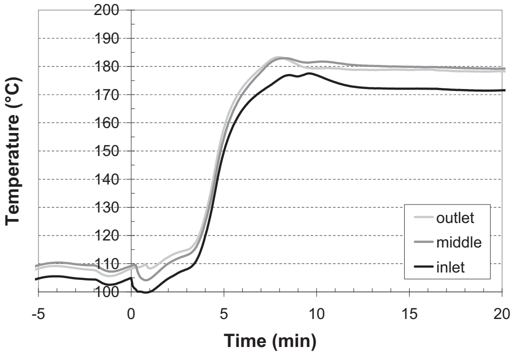 <br>110°C & 180°C |
| 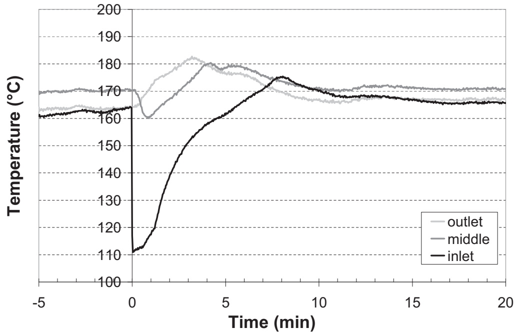 <br>170°C | 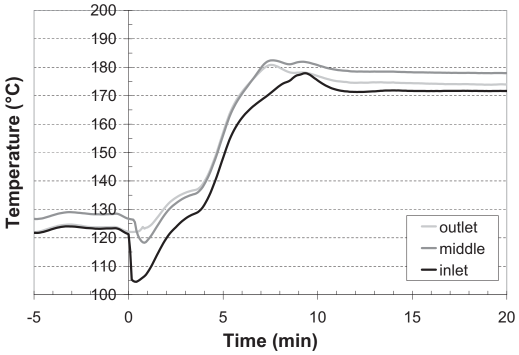 <br>130°C & 180°C |
| 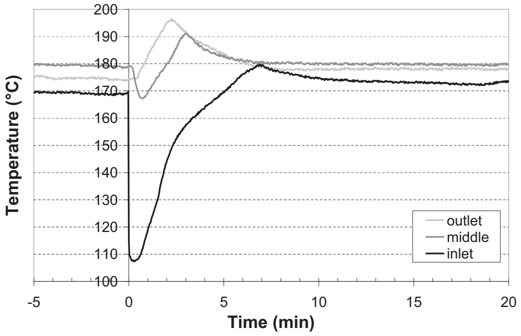 <br>180°C | 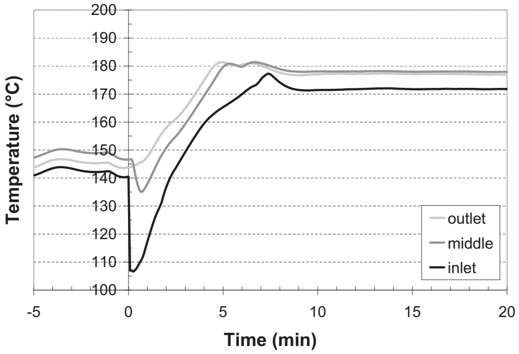 <br>150°C & 180°C |

Figure 5.5 Infusion temperature profiles of the non-isothermal process & the double step process. Infusion & polymerisation temperatures.

# CONCLUSION

In this thesis a literature review on the anionic polyamide-6 glass fibre composites was first presented. Then, the proprietary Ten Cate glass fibre finish 8225 was studied and benchmarked against the 8207 finish to know if it was compatible with APA-6. Results showed that the finish 8225 is not better or worst than the 8207, but it is certainly compatible with an APA-6 system.

Afterwards, two heating set-ups, the platen press and the radiative, were compared. It was shown that the radiative set-up yielded better quality laminates based on ILSS because its heating surface covers the complete laminate and mould. When using a mould temperature of 180°C, the interlaminar shear strength was maximised, this curing temperature was selected for a second study in which a double step infusion strategy was tested.

The double step infusion strategy was tested with different infusion temperatures. The infusion temperature of 110°C and 130°C produced the most uniform laminates based on their interlaminar shear strength and melt temperature standard deviation. Also, ultrasonic testing and microscopy confirmed the uniform quality of these laminates. Furthermore, this processing strategy using a 150°C infusion temperature increased the melt temperature when compared to composites produced with a non-isothermal infusion strategy at equivalent polymerisation temperature. Finally, because of its ability to better controlling the polymerisation exothermic peaks, the double step infusion strategy yielded more uniform laminates when compared to the non-isothermally produced composites.

Hopefully one days, all the products made on Earth will be (reduced, reused and) recyclable. The thermoplastic composites development is crucial to be able to live in a sustainable industrialised society. Even wind turbine blades, which produce clean and green energy, can be made with these materials. It is in this context that the author wishes to see more research performed toward manufacturing goods made with APA-6 composites.

# RECOMMENDATION

To continue improving the quality of fibre reinforced APA-6 composites, recommendations are made.

## Methodology issues

1.1 Since voids alters the laminate mechanical properties, it is proposed to test and analyse only laminates free of voids. Through the laminates manufacturing, it has been seen that it is difficult to manufacture only laminates free of voids. Therefore, it is also suggest to make extra efforts to manufacture enough laminates free of voids.

1.2 The sample population of the data presented in chapter 5 is low, since only one laminate was tested on ILSS for each infusion temperature. It is suggested to have a larger population like three laminates free of voids for each tested infusion temperatures.

## Manufacturing issues

2.1 In some occasions through the experiments, the APA-6 solution in the buffer vessel gained too much viscosity to be infused. The matrix solution polymerised too fast, *i.e.* the pot life was too short at 110℃. To solve this problem, it is suggested that the matrix solution should to be held at a lower temperature than 110℃ but higher than 69℃ (the caprolactam melt temperature). Maybe 90℃ could be a good temperature for the MMU tanks and buffer vessel. Hedrick *et al.* from Monsanto suggest that "some catalyst-initiator systems, such as the alkyl magnesium chloride-acetyl caprolactam system, will require even a further reduction in heat to less than 80°C to prevent polymerisation" [94].

2.2 The present APA-6 system is very sensitive to moisture. Throughout the experiments, many laminates have shown signs of bad polymerisation. To minimise the effect of moisture on processing, actions are suggested to control the atmospheric humidity. It is suggested to use special equipment like a glovebox or to work in a temperature and humidity controlled room.

2.3 To minimise the moulding cycle time, the crystallisation temperature should be investigated because the crystallisation rate is a function of the mould temperature. By modifying the moulding temperature from the polymerisation temperature, 180℃, to a lower crystallisation temperature, 138℃, the crystallisation rate could be maximise, thus potentially reducing overall processing time [67, 70].

2.4 The controller's thermocouples should always be located inside the laminate to get exactly the desired set-point temperature at the outlet. This position will also allow the controllers to take into account the heat produced by the APA-6 exothermic polymerisation reaction. This issue will be especially important when producing thick laminates.

### Interphase issues

3.1 Since, the 180℃ non-isothermal ILSS is higher than the 150 – 180℃ double step ILSS, it is suggested to study again the polymerisation temperature to enhance the ILSS. It would be interesting to try a polymerisation temperature of 195℃, because it is close to the exothermic peak of the 180℃ non-isothermal laminates, 196.46℃.

3.2 To understand the interphase morphology and therefore the relation between the $X_c$ and the ILSS, the coupling agent of the proprietary 8225 finish has to be known. Furthermore, an interphase micrographics study, such as the one performed by Bessel *et al.* [86] could be beneficial. The fibre coupling agent and the moulding temperature affect the interphase which can be composed of different polymorph possibilities, *i.e.* amount, nature and orientation of crystals. Thus, it is proposed to quantify each APA-6 crystals phases, mainly $\alpha$ & $\gamma$, since the polymerisation temperature can influence the crystal phases formation [61]. The wide-angle X-ray scattering (WAXS) could be used to distinguish these phases [120–123].

3.3 To enhance even more the interphase, a study on various fibre coupling agents could be done. Coupling agents from table 1.5 & 1.6 could be investigated. Others coupling agents could be coated on fibres with a silane coupling agent ($\gamma$-aminopropyltriethoxysilane) linked to a low molecular weight blocked polyisocyanates. The silane could potentially bond with the glass fibre surfaces and the blocked isocyanate could unblocked above 150℃ to branched with the APA-6 chains [124, 125].

3.4 The incorporation of an organosilicon to the monomer solution could potentially increase the interphase properties. In that case, a silane molecule would end the APA-6 polymer chain. Also, this amino silane could be used to control the molecular weight and to produce more uniform linear polymer with less cyclic polyamides. Unfortunately, using this approach, the catalytic system would have to be revised. If the added organosilicon contains an isocyanate, then it could possibly replace the activator [91].

### Tests issues

4.1 To be more time effective, the thermal gravimetric analysis (TGA) is suggested to determine the DOC. With the same TGA test, $W_f\%$ could also be determine [7, 126]. Time could be saved even more by using a machine that can do TGA and DSC simultaneously. Therefore, the $T_m$, $X_c$, DOC and $W_f\%$ could be determine simultaneously in a reliable manner.

### Processing strategy issue

5.1 To incorporate some of the above recommendations, a new multi steps infusion strategy is suggested, see figure 5.6. It is based on the double step strategy but will include two more steps. To keep a low polymerisation rate, the infusion is made at 95℃. After infusion, the mould temperature could be raised to the de-blocking temperature (150℃), to let the activator de-block and link itself to the fibre coupling agent.

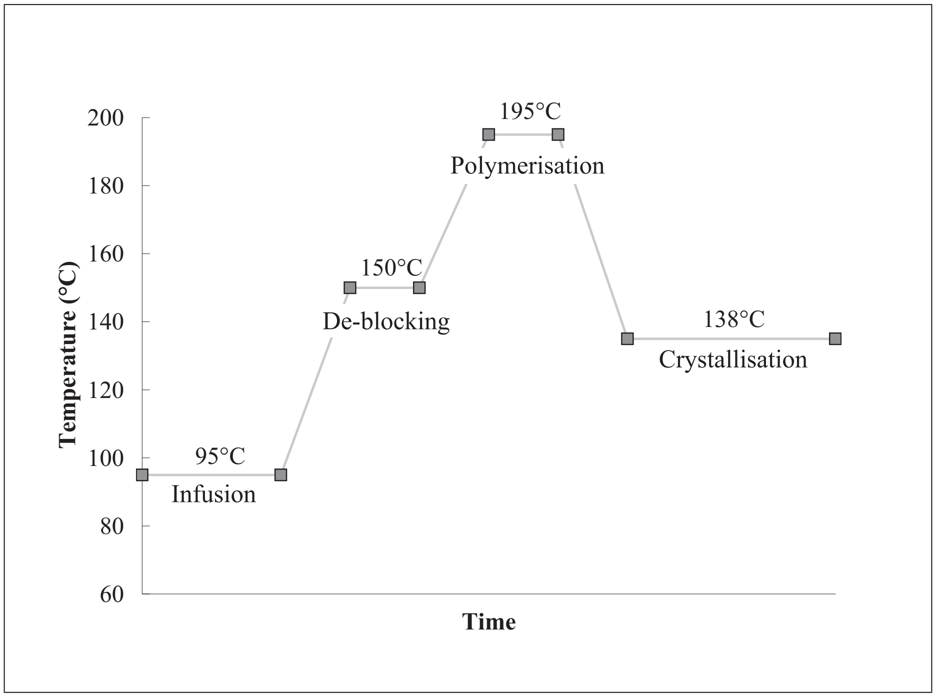

Figure 5.6 Multi step infusion strategy.

After, the mould temperature could again be increased to a polymerisation temperature (195℃), to optimise the ILSS. Finally to efficiently develop the crystal phases, the mould temperature could be dropped to an optimum crystallisation temperature (138℃). All these steps have a different elapsed time that would need to be studied to achieve the best composite performance.

# BIBLIOGRAPHY

[1] European Union. Directive 2000/53/ec of the european parliament and of the concil: end-of life vehicles, 21 October 2000.

[2] National Materials Advisory Board (NAS-NAE). The place for thermoplastic composites in structural components. Technical Report NMAB-434, National Research Council, Commission On Engineering and Technical Systems, Washington DC, 1987.

[3] J. Verrey, M. D. Wakeman, V. Michaud, and J. A. E. Månson. Manufacturing cost comparison of thermoplastic and thermoset rtm for an automotive floor pan. *Composites Part A: Applied Science and Manufacturing*, 37(1):9–22, 2006.

[4] W. D. Brouwer, E. F. C. F. van Herpt, and M. Labordus. Vacuum injection moulding for large structural applications. In *Compos. A, Appl. Sci. Manuf. (UK)*, volume 34A, pages 551–8, UK, 2003. Elsevier.

[5] K. van Rijswijk and H. E. N. Bersee. Reactive processing of textile fiber-reinforced thermoplastic composites - an overview. *Composites Part A: Applied Science and Manufacturing*, 38(3):666–681, 2007.

[6] K. Van Rijswijk, S. Joncas, H. E. N. Bersee, and O. K. Bergsma. Vacuum infused fiber-reinforced thermoplastic mw-size turbine blades: A cost-effective innovation? In *43rd AIAA Aerospace Sciences Meeting and Exhibit - Meeting Papers*, pages 15307–15319, Reno, NV, 2005. American Institute of Aeronautics and Astronautics Inc., USA.

[7] Selvum Pillay, Uday K. Vaidya, and Gregg M. Janowski. Liquid molding of carbon fabric-reinforced nylon matrix composite laminates. *Journal of Thermoplastic Composite Materials*, 18(6):509–527, 2005.

[8] Harald E.N. Bersee Julie J. E. Teuwen, Jac H.A.M. Gillis. Optimisation of infusion temperature for anionic polyamide-6 composites. In *Structures, Structural Dynamics, and Materials Conference*, Schaumburg, IL, 2008. American Institute of Aeronautics and Astronautics.

[9] K. van Rijswijk, J. J. E. Teuwen, H. E. N. Bersee, and A. Beukers. Textile fiber-reinforced anionic polyamide-6 composites. part I: The vacuum infusion process. *Composites Part A: Applied Science and Manufacturing*, 40(1):1–10, 2009.

[10] Tony Burton, David Sharpe, Nick Jenkins, and Ervin Bossanyi. *WIND ENERGY HANDBOOK.* John Wiley & Sons, Chichester, West Sussex, England, 2001.

[11] M. M. Shokrieh and R. Rafiee. Simulation of fatigue failure in a full composite wind turbine blade. *Composite Structures*, 74(3):332–42, 2006.

[12] C. Berggreen, K. Branner, J. F. Jensen, and J. P. Schultz. Application and analysis of sandwich elements in the primary structure of large wind turbine blades. *Journal of Sandwich Structures and Materials*, 9(6):525–552, 2007.

[13] Charles A. Harper. *Modern Plastics Handbook*. McGraw-Hill, New York, USA, 2000.

[14] J. A. Brydson. *Plastics Materials*. Butterworth-Heinemann, Jordan Hill, Oxford, UK, $7^{\text{th}}$ edition, 1999.

[15] R.J. Crawford. *PLASTICS ENGINEERING*. Butterworth-Heinemann, Jordan Hill, Oxford, UK, $3^{\text{th}}$ edition, 1998.

[16] Lawrence Drzal. The interphase in epoxy composites. In K. Dušek, editor, *Epoxy Resins and Composites II*, pages 1–32. Springer Berlin / Heidelberg, 1986.

[17] Lawrence T. Drzal, Michael J. Rich, and Pamela F. Lloyd. Adhesion of graphite fibers to epoxy matrices: I. the role of fiber surface treatment. *Journal of Adhesion*, 16(1):1–30, 1983.

[18] Jang-Kyo Kim and Yiu-Wing Mai. *Engineered interfaces in fiber reinforced composites*. Elsevier science Ltd, Oxford, UK, 1998.

[19] Harry E. Pebly. Glossary of terms. In Theodore J. Reinhart, editor, *Composites*, volume 1 of *Engineered materials Handbook*, page 983. ASM International, Metals Park, Ohio, 1987.

[20] Michael James Owen. Coupling agents: Chemical bonding at interfaces. In M. Chaudhury and A. V. Pocius, editors, *Surfaces, Chemistry and Applications*, volume 2, pages 403–431. Elsevier Science B.V., Amsterdam, 2002.

[21] M. W. Ranney, S. E. Berger, and J. G. Marsden. Silane coupling agent in particulate mineral filled composites. In Edwin P. Plueddemann, editor, *Interfaces in polymer matrix composites*, volume 6 of *Composite materials*. Lawrence J. Broutman and Richard H. Krock, series editors. Acamedic press, New York, 1974.

[22] Edwin P. Plueddemann. Mechanism of adhesion through silane coupling agents. In Edwin P. Plueddemann, editor, *Interfaces in polymer matrix composites*, volume 6 of *Composite materials*. Lawrence J. Broutman and Richard H. Krock, series editors. Acamedic press, New York, 1974.

[23] Edwin P. Plueddemann. *Silane coupling agents*. Plenum press, New York, $2^{\text{nd}}$ edition, 1991.

[24] M. J. Pitkethly, J. P. Favre, U. Gaur, J. Jakubowski, S. F. Mudrich, D. L. Caldwell, L. T. Drzal, M. Nardin, H. D. Wagner, L. Di Landro, A. Hampe, J. P. Armistead, M. Desaeger, and I. Verpoest. A round-robin programme on interfacial test methods. *Composites Science and Technology*, 48(1-4):205–214, 1993.

[25] Arlen Hoebergen and J. Anders Holmberg. Vacuum infusion. In Daniel. B. Miracle and Steven L. Donaldson, editors, *Composites*, volume 21 of *ASM Handbook*, page 1188. ASM International, Materials Park, Ohio, 2001.

[26] Adriaan Beukers and Ed van Hinte. *Lightness: the inevitable renaissance of minimum energy structures.* 010 publishers, Rotterdam, 4th edition, 2005.

[27] Douglas S. Cairns and Jon D. Shramstad. Evaluation of hand lay-up and resin transfer molding in composite wind turbine blade manufacturing. Technical Report SAND2000-1425, Sandia National Laboratories, 2000.

[28] Dayton A. Griffin and Thomas D. Ashwill. Blade System Design Studies Volume I: Composite Technologies for Large Wind Turbine Blades. Technical Report SAND2002-1879, Sandia National Laboratories, 2002.

[29] Dayton A. Griffin. Blade system design studies volume II : preliminary blade designs and recommended test matrix. Technical Report SAND2004-0073, Sandia National Laboratories, 2004.

[30] Povl Brøndsted, Hans Lilholt, and Aage Lystrup. Composite materials for wind power turbine blades. *Annual Review of Materials Research*, 35(1):505–538, 2005.

[31] Aage Lystrup. Vacuum consolidation of thermoplastic composites for wind turbine rotor blades. In H.Lilholt B.Madsen T.L.Andersen L.P.Mikkelsen & A.Thygesen, editor, *Polymer Composite Materials for Wind Power Turbines*, pages 231–238, Denmark, 2006. Risø National Laboratory.

[32] Kamal J Araj, Theresa A. Fisher, and Jan C. Kronenburg. Assessment of research needs for wind turbine rotor materials technology. Technical report, National Research Council, 1991.

[33] Dayton A. Griffin. Cost / performance tradeoffs for carbon fiber in wind turbine blades. In *Sandia Blade Technology Workshop*, 2004.

[34] Irving E. Muskat. Method of molding. United States patent office no. 2495640, 1950.

[35] Christopher Williams, John Summerscales, and Stephen Grove. Resin infusion under flexible tooling (rift): a review. *Composites Part A: Applied Science and Manufacturing*, 27(7):517–524, 1996.

[36] D. Cripps, T. J. Searle, and J. Summerscales. Open mold techniques for thermoset composites. In Kelly Anthony and Zweben Carl, editors, *Polymer matrix composites*, volume 2 of *Comprehensive Composite Materials*, pages 737–761. Pergamon, Oxford, 2000.

[37] F.C. Campbell. *Manufacturing Processes for Advanced Composites.* Elsevier Advanced Technology, Oxford, UK., 2004.

[38] Henri Philibert Gaspard Darcy. *Les fontaines publiques de la ville de Dijon : exposition et application des principes a suivre et des formules a employer dans les questions de distribution d'eau : ouvrage terminé par un appendice relatif aux fournitures d'eau de plusieurs villes au filtrage des eaux et a la fabrication des tuyaux de fonte, de plomb, de tole et de bitume.* Victor Dalmont, Libraire des Corps imperiaux des ponts et chaussées et des mines, Paris, 1856.

[39] M. Marle, C. Henry darcy et les écoulements de fluides en milieu poreux. *Oil & Gas Science and Technology - Rev. IFP*, 61(5):599–609, 2006.

[40] George Lubin (editor). *Handbook of composites.* Van Nostrand Reinhold company Inc., New York, USA, 1st edition, 1982.

[41] Patrick J. Mallon and Conchúr M. ÓBrádaigh. Compliant mold techniques for thermoplastic composites. In Kelly Anthony and Zweben Carl, editors, *Polymer matrix composites*, volume 2 of *Comprehensive composite materials*, pages 873–913. Pergamon, Oxford, 2000.

[42] Christopher Macosko. *RIM Fundamentals of reaction injection molding.* Hanser, Munich, 1989.

[43] P. E. Bourban. Liquid molding of thermoplastic composites. In Kelly Anthony and Zweben Carl, editors, *Polymer matrix composites*, volume 2 of *Comprehensive composite materials*, pages 965–977. Pergamon, Oxford, 2000.

[44] C. Li Pi Shan, W. E. Baker, M. F. Cunningham, and M. C. Baird. Conversion studies in a novel reaction injection molding process for syndiotactic polystyrene. *Journal of Applied Polymer Science*, 70(13):2679–2693, 1998.

[45] M. Grujicic, K. M. Chittajallu, and S. Walsh. Optimization of the vartm process for enhancement of the degree of devolatilization of polymerization by-products and solvents. *Journal of Materials Science*, 38(18):3729–3739, 2003.

[46] Niccolo Pini, Chiara Zaniboni, Stephan Busato, and Paolo Ermanni. Perspectives for reactive molding of ppa as matrix for high-performance composite materials. *Journal of Thermoplastic Composite Materials*, 19(2):207–216, 2006.

[47] Alex Tullo. Best of both worlds, cyclic corp. hopes that a new twist on polybutylene terephthalate will create a niche. *Chemical & engineering news*, 80(44):22, 2002. On line. "`http://pubs.acs.org/cen/coverstory/8044/print/8044companies5.html`". Last checked: November 17, 2009.

[48] Fulcrum Thermoplastic composite technology, 2005. On line. "`http://fulcrumcomposites.com/`". Last checked: November 18, 2009.

[49] DSM. Ap-caprolactam for cast nylon, 2009. On line. "`http://www.dsm.com/en_US/html/dfi/ap.htm`". Last checked: November 18, 2009.

[50] BrüggemannChemical. Ap-nylon$^{®}$ materials, 2009. On line. "`http://www.brueggemann.com/english/ap-nylon-produkte.html`". Last checked: November 18, 2009.

[51] P. Ó Máirtín, P. McDonnell, M. T. Connor, R. Eder, and C. M. Ó Brádaigh. Process investigation of a liquid pa-12/carbon fibre moulding system. *Composites Part A: Applied Science and Manufacturing*, 32(7):915–923, 2001.

[52] K. van Rijswijk. *Thermoplastic Composite Wind Turbine Blades: Vacuum Infusion Technology for Anionic Polyamide-6 Composites*. PhD thesis, Delft University of Technology, 2007.

[53] Stefan Czernik, Carolyn C. Elam, Robert J. Evans, Robert R. Meglen, Luc Moens, and Kuniyasu Tatsumoto. Catalytic pyrolysis of nylon-6 to recover caprolactam. *Journal of Analytical and Applied Pyrolysis*, 46(1):51–64, 1998.

[54] Marc-André Beauchamp, Simon Joncas, and H.E.N. Bersee. Vacuum infused anionic polyamide-6 composites: The development of a recycling strategy. In *Sampe 2010: New materials and processs for new econnomy*, Washington, USA, 2010.

[55] Wallace H. Carothers. Linear condensation polymers. United States patent office no. 2071250, February 1937.

[56] Paul Matthies and Wolfgang F. Seydl. History and development of nylon 6. In *High Performance Polymers: Their Origin and Development, Proceedings of the Symposium. Presented at the 91st Meeting of the American Chemical Society.*, pages 39–53, New York, NY, USA, 1986. Elsevier.

[57] K. van Rijswijk, S. Lindstedt, D. P. N. Vlasveld, H. E. N. Bersee, and A. Beukers. Reactive processing of anionic polyamide-6 for application in fiber composites: A comparitive study with melt processed polyamides and nanocomposites. *Polymer Testing*, 25(7):873–887, 2006.

[58] Herbert K. Reimschuessel. Nylon 6. chemistry and mechanisms. *Journal of Polymer Science: Macromolecular Reviews*, 12(1):65–139, 1977.

[59] K. Udipi, R. S. Dave, R. L. Kruse, and L. R. Stebbins. Polyamides from lactams via anionic ring-opening polymerization. 1. chemistry and some recent findings. *Polymer*, 38(4):927–938, 1997.

[60] O. Wichterle, J. Sebenda, and J. Králícek. The anionic polymerization of caprolactam. In *Fortschritte Der Hochpolymeren-Forschung*, pages 578–595. Springer Berlin / Heidelberg, 1961.

[61] Laura Ricco, Saverio Russo, Giustino Orefice, and Fernando Riva. Anionic poly($\varepsilon$-caprolactam): Relationships among conditions of synthesis, chain regularity, reticular order, and polymorphism. *Macromolecules*, 32(23):7726–7731, 1999.

[62] W. E. Hanford and R. M. Joyce. Polymeric amides from epsilon-caprolactam. *Journal of Polymer Science*, 3(2):167–172, 1948.

[63] H. K. Hall. Structural effects on the polymerization of lactams. *Journal of the American Chemical Society*, 80(23):6404–6409, 1958.

[64] M. Hedrick R, D. Gabbert J, and H. Wohl M. Nylon 6 rim. In *Reaction Injection Molding*, ACS Symposium Series, pages 135–162. American Chemical Society, Washington, D.C., 1985.

[65] Jaroslav Stehlicek and Rudolf Puffr. Anionic polymerization of 6-hexanelactam, 62. fast catalytic systems in the anionic polymerization of 6-hexanelactam. *Die Makromolekulare Chemie*, 193(10):2539–2545, 1992.

[66] Kazue Ueda, Kazunobu Yamada, Makoto Nakai, Tsunetoshi Matsuda, Masahiro Hosoda, and Kazuo Tai. Synthesis of high molecular weight nylon 6 by anionic polymerization of $\varepsilon$-caprolactam. *Polymer Journal*, 28(5):446–451, 1996.

[67] J. H. Magill. Crystallization kinetics study of nylon 6. *Polymer*, 3:655–664, 1962.

[68] T. M. Frunze, R. B. Shleifman, E. M. Belavtseva, Ya V. Genin, T. V. Volkova, V. A. Kotel'nikov, L. G. Radchenko, S. P. Davtyan, V. V. Kuraschev, and D. Ya Tsvankin. Kinetic studies of structure formation during anionic adiabatic polymerization of $\varepsilon$-caprolactam. *Journal of Polymer Science, Polymer Physics Edition*, 18(7):1523–1532, 1980.

[69] H. Ishida and C. Scott. Fast polymerization and crystallization kinetic studies of nylon 6 by combined use of computerized micro-rim machine and ft-ir. *Journal of Polymer Engineering*, 6(1-4):201–217, 1986.

[70] Stanley A. Iobst. Polymerization and crystallization behavior of anionic nylon 6. *Polymer Engineering & Science*, 25(7):425–430, 1985.

[71] Steffen Maier, Ton Loontjens, Boudewijn Scholtens, and Rolf Mülhaupt. Carbonylbiscaprolactam: A versatile reagent for organic synthesis and isocyanate-free urethane chemistry. *Angewandte Chemie International Edition*, 42(41):5094–5097, 2003.

[72] John Hee Hong, Chang Woo Choi, S. Ramasundaram, A. Anand Prabu, Jong Soon Lee, Kap Jin Kim, Jun Ho Yang, and Dong Jun Lee. Studies on the recycling of glycolyzed nylon 66 using novel chain extenders. *Polymer Degradation and Stability*, 93(2):392–400, 2008.

[73] Jan Roda. Polyamides. In P. Dubois, O. Coulembier, and J.-M. Raquez, editors, *Handbook of Ring-Opening Polymerization*, pages 165–195. WILEY-VCH Verlag GmbH & Co. KGaA, 2009.

[74] Gh. Rusu, K. Ueda, E. Rusu, and M. Rusu. Polyamides from lactams by centrifugal molding via anionic ring-opening polymerization. *Polymer*, 42(13):5669–5678, 2001.

[75] G. B. Gechele and G. Stea. Heterogeneous polymerization of $\varepsilon$-caprolactam. *European Polymer Journal*, 1(2):91–102, 1965.

[76] T. Bessell and J. B. Shortall. The effect of polymerization variables on the induction time and morphology of polycaprolactam. *European Polymer Journal*, 8(8):991–998, 1972.

[77] Carlo Giovanni Alfonso, Carmen Chiappori, Sandro Razore, and Saverio Russo. Activated anionic polymerization of $\varepsilon$-caprolactam for rim process. In *Reaction Injection Molding*, ACS Symposium Series, pages 163–179. American Chemical Society, Washington, D.C., 1985.

[78] T. J. Bessell, D. Hull, and J. B. Shortall. The effect of polymerization conditions and crystallinity on the mechanical properties and fracture of spherulitic nylon 6. *Journal of Materials Science*, 10(7):1127–36, 1975.

[79] K. van Rijswijk, H. E. N. Bersee, A. Beukers, S. J. Picken, and A. A. van Geenen. Optimisation of anionic polyamide-6 for vacuum infusion of thermoplastic composites: Influence of polymerisation temperature on matrix properties. *Polymer Testing*, 25(3):392–404, 2006.

[80] K. van Rijswijk, H. E. N. Bersee, W. F. Jager, and S. J. Picken. Optimisation of anionic polyamide-6 for vacuum infusion of thermoplastic composites: choice of activator and initiator. *Composites Part A: Applied Science and Manufacturing*, 37(6):949–956, 2006.

[81] B. L. Hollingsworth. New fibre-filled thermoplastics part 1 – the future for asbestos. *Composites*, 1(1):28–34, 1969.

[82] B. L. Hollingsworth and D. Sims. New fibre-filled thermoplastics part 2–reinforcement by high modulus fibres. *Composites*, 1(2):80–86, 1969.

[83] Robert E. Miller. Reinforced polyamides containing phosphorus coupling agents and processes therefor. United States patent office no. 3344107, September 1967.

[84] Ross M. Hedrick and William R. Richard Jr. Reinforced polyamides and process of preparation thereof. United States patent office no. 3419517, December 1968.

[85] T. Bessell, D. Hull, and J. B. Shortall. Uniaxially aligned fibre reinforced nylon composites. *Nature (Physical Science)*, 232:127–9, 1971.

[86] T. Bessell, D. Hull, and J. B. Shortall. Interface morphology and mechanical properties of unidirectional fibre reinforced nylon 6. *Special Discussions of the Faraday Society*, 2:137, 1972.

[87] Morton H. Litt and Allan W. Brinkmann. Nylon 6/graphite fiber composites by in situ polymerization. *Journal of Elastomers and Plastics*, 5(3):153–160, 1973.

[88] T. Bessell and J. B. Shortall. The crystallization and interfacial bond strength of nylon 6 at carbon and glass fibre surfaces. *Journal of Materials Science*, 10(12):2035–2043, 1975.

[89] T. J. Bessell and J. B. Shortall. The mechanical properties and fracture behaviour of unidirectionally reinforced nylon 6. *Journal of Materials Science*, 12(2):365–372, 1977.

[90] Lloyd A. Goettler and Willard J. Neff. Mechanical performance of various nylon 6 composites formed by *in-situ* polymerization of caprolactam. *Polymer Composites*, 7(5):383–394, 1986.

[91] Ross M. Hedrick and William R. Richard Jr. Polyamides containing silane end groups. United States patent office no. 3341501, September 1967.

[92] Jr. William R. Richard. Reinforced polyamide compositions and process of preparation thereof. United States patent office no. 3833534, September 1974.

[93] Ross M. Hedrick, Paul A. Tierney, and William R. Richard Jr. Process for polymerizing lactams in the presence of filler or reinforcing agent. United States patent office no. 3386943, June 1968.

[94] Ross Melvin Hedrick and William R. Richard Jr. Reinforced polyamides and process of preparation thereof. United States patent office no. RE28646, December 1975.

[95] L. W. Jenneskens, H. E. C. Schuurs, D. J. Simons, and L. Willems. Molecular mechanisms of adhesion promotion by silane coupling agents in glass bead-reinforced polyamide-6 model composites. *Composites*, 25(7):504–511, 1994.

[96] K. van Rijswijk, A. A. van Geenen, and H. E. N. Bersee. Textile fiber-reinforced anionic polyamide-6 composites. part II: Investigation on interfacial bond formation by short beam shear test. *Composites Part A: Applied Science and Manufacturing*, 40(8):1033–1043, 2009.

[97] Deepika Chandrakant Shah. In situ molding of glass fibre/nylon 6 composites: Studies in the development of composite properties by surface modification of glass fibre. Master's thesis, University of Alberta (Canada), 1996.

[98] Suk Hyang Yun, Donghwan Cho, Junkyung Kim, Soonho Lim, Geon-Woong Lee, Min Park, and Sang-Soo Lee. Effect of silane coupling agents with different organofunctional groups on the interfacial shear strength of glass fiber/nylon 6 composites. *Journal of Materials Science Letters*, 22(22):1591–1594, 2003.

[99] D. Cho, S. H. Yun, J. Kim, S. Lim, M. Park, S. S. Lee, and G. W. Lee. Influence of silane coupling agents on the interlaminar and thermal properties of woven glass fabric/nylon 6 composites. *Macromolecular Research*, 12(1):119–126, 2004.

[100] Ward T. Collins and Jari L. Kludt. Silane coupling agents for silane-treated mineral reinforced engineering thermoplastics. *Plastics Design & Processing*, 16(February):12–15, 1976.

[101] Edwin P. Plueddemann. Composites having ionomer bonds with silanes at the interface. *Journal of Adhesion Science and Technology*, 3(2):131–139, 1989.

[102] Ulrike Lechner and Rudolf Kruedener. Polyamide reinforced with silanized glass fibers. United States patent office no. 5240974, August 1993.

[103] S. Joncas, K. Van Rijswijk, J. F. Charron, H. E. N. Bersee, and A. Beukers. Interfacial shear strength properties of vacuum-infused anionic polyamide-6 glass-fiber composites. In *AIAA/ASME/ASCE/AHS/ASC Structures, Structural Dynamics and Materials Conference*, volume 11, pages 7862–7869, Newport, RI, United States, 2006. American Inst. Aeronautics and Astronautics Inc.

[104] J. U. Otaigbe. Effect of coupling agent and absorbed moisture on the tensile properties of a thermoplastic rrim composite. *Journal of Applied Polymer Science*, 45(7):1213–1221, 1992.

[105] Apinya Duangchan. Glass fibre and nylon 6: An advanced composite material. Master's thesis, University of Alberta (Canada), 1994.

[106] Edwin P. Plueddemann. Adhesion through silane coupling agents. *The Journal of Adhesion*, 2(3):184 – 201, 1970.

[107] Edwin P. Plueddemann. Cationic silane coupling agents for thermoplastics. *Polymer-Plastics Technology and Engineering*, 2(1):89–106, 1973.

[108] Paul Marx, C. W. Smith, A. E. Worthington, and Malcolm Dole. Specific heat of synthetic high polymers. iv. polycaprolactam. *The Journal of Physical Chemistry*, 59(10):1015–1019, 1955.

[109] M. Dole and B. Wunderlich. Melting points and heats of fusion of polymers and copolymers. *Die Makromolekulare Chemie*, 34(1):29–49, 1959.

[110] Y. P. Khanna and W. P. Kuhn. Measurement of crystalline index in nylons by DSC: Complexities and recommendations. *Journal of Polymer Science Part B: Polymer Physics*, 35(14):2219–2231, 1997.

[111] ASTM International. *Standard Test Methods for Short-Beam Strength of Polymer Matrix Composite Materials and Their Laminates*, volume D 2344 - 00 (Reapproved 2006). ASTM International, 2006.

[112] Melvin I. Kohan. *Nylon Plastics Handbook*. Hanser, 1995.

[113] Shaul M. Aharoni. *n-Nylons: Their Synthesis, Structure and Properties*. Jonh Wiley & Son Ltd, 1997.

[114] industries UBE. Upilex-r thermal control films, 2002.

[115] P. T. Tsilingiris. Comparative evaluation of the infrared transmission of polymer films. *Energy Conversion and Management*, 44(18):2839–2856, 2003.

[116] Watlow. Raymax® 1120-lightweight, sturdy radiant heater panel, 2001.

[117] Kenneth J. Bowles and Stephen Frimpong. Void effects on the interlaminar shear strength of unidirectional graphite-fiber-reinforced composites. *Journal of Composite Materials*, 26(10):1487–1509, 1992.

[118] Michael R. Wisnom, Tom Reynolds, and Nigel Gwilliam. Reduction in interlaminar shear strength by discrete and distributed voids. *Composites Science and Technology*, 56(1):93–101, 1996.

[119] H. Jeong. Effects of voids on the mechanical strength and ultrasonic attenuation of laminated composites. *Journal of Composite Materials*, 31(3):276–292, 1997.

[120] R. F. Stepaniak, A. Garton, D. J. Carlsson, and D. M. Wiles. The characterization of nylon 6 filaments by x-ray diffraction. *Journal of Applied Polymer Science*, 23(6):1747–1757, 1979.

[121] Helen C. Y. Cartledge and Caroline A. Baillie. Studies of microstructural and mechanical properties of nylon/glass composite part I the effect of thermal processing on crystallinity, transcrystallinity and crystal phases. *Journal of Materials Science*, 34(20):5099–5111, 1999.

[122] R. Mateva, P. Petrov, S. Rousseva, R. Dimitrov, and G. Zolova. On the structure of poly-$\varepsilon$-caprolactams, obtained with bifunctional n-carbamyl derivatives of lactams. *European Polymer Journal*, 36(4):813–821, 2000.

[123] T. D. Fornes and D. R. Paul. Crystallization behavior of nylon 6 nanocomposites. *Polymer*, 44(14):3945–3961, 2003.

[124] Christoph Tiburtius, Anna Marx, Hans-ulrich Buschhaus, and Kurt Findeisen. Sizing agent for glass fibers. United States patent office no. 4659753, April 1987.

[125] Marc Cossement, Nadia Masson, and Willy Piret. Size composition. United States patent office no. 5236982, August 1993.

[126] Cai-Liang Zhang, Lian-Fang Feng, and Guo-Hua Hu. Anionic polymerization of lactams: A comparative study on various methods of measuring the conversion of $\varepsilon$-caprolactam to polyamide 6. *Journal of Applied Polymer Science*, 101(3):1972–1981, 2006.